

# Integrating road traffic externalities through a Sustainability Indicator

Fernandes P. <sup>a\*</sup>, Vilaça, M. <sup>a</sup>, Macedo, E. <sup>a</sup>, Sampaio, C. <sup>a</sup>, Bahmankhah, B. <sup>a</sup>, Bandeira, J.M. <sup>a</sup>,  
Guarnaccia, C. <sup>b</sup>, Rafael, S. <sup>c</sup>, Fernandes A.P. <sup>c</sup>, Relvas H. <sup>c\*</sup> Borrego, C. <sup>c</sup>, Coelho, M.C. <sup>a</sup>

<sup>a</sup> Department of Mechanical Engineering / Centre for Mechanical Technology and Automation (TEMA),  
University of Aveiro, Campus Universitário de Santiago, 3810-193 Aveiro – Portugal

<sup>b</sup> Department of Civil Engineering, University of Salerno, Via Giovanni Paolo II, 132, I-84084 Fisciano  
(SA) – Italy

<sup>c</sup> Department of Environment / Centre for Environmental and Marine Studies (CESAM), University of Aveiro,  
Campus Universitário de Santiago, 3810-193 Aveiro - Portugal

\*Assistant Researcher, Mechanical Engineering, E-mail: [paulo.fernandes@ua.pt](mailto:paulo.fernandes@ua.pt)

## ABSTRACT

Road traffic poses negative externalities on society and represents a key challenge in sustainable transportation.

This paper develops a sustainability indicator that integrates traffic-related externalities as means of traffic congestion, noise, greenhouse gases (GHG) and nitrogen oxides emissions, health impacts and road crash related costs, and adjusted to local contexts of vulnerability.

Traffic, road crashes, acoustic and vehicle dynamic data were collected from one real-world intercity corridor pair comprising three alternative routes. The site-specific operations were characterized using a modeling platform of traffic, emissions, noise and air quality. A specific methodology is applied for each road traffic externality and translated in a single factor – external cost.

The results indicated that road crashes presented the largest share in the partly rural/urban route while GHG emissions had the highest contribution in external costs for the highway routes. Also, the distribution of external cost component varied according to the type of road, mostly due to different levels of exposed inhabitants.

36 This paper offers a line of research that produced a method for decision-makers with  
37 reliable and flexible cost analysis aimed at reducing the negative impacts of road traffic. It  
38 also encourages the design of eco-traffic management policies considering the perspective  
39 of drivers, commuters, population and system.

40 *Keywords:* Sustainability Indicator, External Costs, Road Traffic, Modeling, Traffic  
41 Externalities.

42

## 43 1. INTRODUCTION AND RESEARCH OBJECTIVES

44 Road traffic poses negative externalities on society, thereby representing one of the key  
45 challenges in sustainable transportation nowadays. In 2016, road transportation accounted  
46 for 73% and 83% of transportation greenhouse gases (GHG) emissions in the European  
47 Union (EU) **(EEA, 2017b)** and in the United States (US) **(EPA, 2018)**, respectively. Long  
48 term-projections for carbon dioxide (CO<sub>2</sub>) emissions concerning the passenger  
49 transportation in cities of over 300 000 inhabitants show an increase up to 27% in 2050  
50 compared with 2015 levels **(Chen and Kauppila, 2017)**.

51 Besides GHG emissions, road transportation has long-lasting negative impacts on road  
52 safety, human health and wellbeing. Road traffic crashes within EU claimed approximately  
53 25,650 fatalities in 2016 **(ERSO, 2018)**; 54% of these occurred at rural roads **(ERSO, 2018)**.

54 Also, road transportation is one of the major sources of some harmful air pollutants such as  
55 particulate matter (PM), nitrogen oxides (NO<sub>x</sub>) and carbon monoxides (CO) **(EEA, 2018a)**.

56 Around 39% of total NO<sub>x</sub> came from road transportation (EU member states), which  
57 represented the highest share of that gas in 2015 **(EEA, 2017a)**. This sector is, by far, the  
58 dominant source of traffic noise in Europe, representing almost 90% of total noise emissions  
59 **(EEA, 2018b)**. Approximately 29 million living in main roads outside urban areas in EU-  
60 28 were exposed to average day-evening-night noise levels ( $L_{den}$ ) exceeding 55 dBA **(EEA,**  
61 **2018b)**. Traffic noise causes nuisance, stress reactions, sleep disturbance, and it also  
62 has negative effects on health, such as cardiovascular diseases **(WHO, 2011)**.

63 Understanding the most cost-effective strategies to mitigate both congestion and  
64 environmental related costs in automobile trips has been pointed out as one of the critical  
65 issue in transportation for the next 20 years **(National Academies of Sciences, 2018)**. The  
66 overall size of transportation external costs is estimated at around 7% of the EU Gross  
67 Domestic Product **(EC, 2018)**. In this context, a more efficient use of existing infrastructure  
68 is essential to reduce road transportation externalities **(EC, 2011)**.

69

70 However, there are some answered questions about the quantification of external costs  
71 namely:

72 • What is would be the cost of a given route if drivers had to pay for their  
73 choices?

74 • Why would a driver have to choose the route with lowest emissions if local  
75 population could be at higher risk exposure to other traffic externalities?

76 • If drivers shift towards a fast route but with high traffic volumes and resulting  
77 pollutant emissions, then what would be the benefits in terms of overall costs  
78 compared to slower routes?

79 For this purpose, a simulation-based approach was conducted combining a methodology  
80 for estimating GHG (CO<sub>2</sub> and Volatile Organic Compounds –VOCs), NO<sub>x</sub> and PM  
81 emissions, air quality (PM concentrations) and noise using a microscopic traffic simulation  
82 tool together with road crashes historical data in a real origin-destination (N-S and S-N) pair  
83 between Aveiro and Estarreja, Portugal. The location comprised three alternative routes,  
84 as follows: *i)* partly rural/urban; *ii)* low-traffic-volume highway with electronic pay tolls; and  
85 *iii)* high-traffic-volume highway with both conventional and electronic pay tolls. The  
86 proposed methodology allows to build a link-based sustainability indicator that can be  
87 updated in real-time through a set of information sources and translated into a monetary  
88 value.

89 This research intends to contribute for decision making by traffic management entities in  
90 the following aspects:

91 • To endow the current navigation platforms with reliable and flexible cost analysis  
92 which takes into account local-specific needs;

93 • To include other variables in order to assess their impact on the magnitude and  
94 share of traffic externalities according to the type of road;

- 95 • To encourage the design of eco-traffic management policies considering the  
96 perspective of drivers, commuters, population and system.

97

98 The remainder of the paper is organized as follows. **Section 2** presents a review of scientific  
99 literature regarding the integration of road traffic externalities. In **Section 3**, the  
100 methodology for traffic, vehicular emissions, air quality and noise modeling, and calibration  
101 and validation of the simulation platform are presented, as well as the procedure for  
102 developing the proposed sustainability indicator. **Section 4** describes the real-world  
103 intercity corridor, data collection and main modeling tasks. Subsequently, the results are  
104 used to assess the sustainable indicator in the candidate case study (**Section 5**). In all  
105 comparisons, the focus will be on range of each cost component value along routes, and  
106 potential trade-off among them. The final section outlines the main research findings and  
107 contributions and points out some future research needs (**Section 6**).

108

## 109 2. LITERATURE REVIEW

110 Internalizing the external costs of transportation has been an important concern for policy  
111 development and transportation research. According to **Korzhenevych et al. (2014)**,  
112 internalization of transportation externalities can be based on quantifying in monetary  
113 values the associated impacts on society and environment, such as congestion, traffic  
114 noise, air pollution, greenhouse effects and road crashes. This degree of damage widely  
115 depends on the geographic conditions, intensity of traffic and population exposed (**Yeh,**  
116 **2013**).

117 Negative externalities in the road transportation sector constitute an important development  
118 issue with socioeconomic costs (**Cecchel et al., 2018**) which are known to lead to welfare  
119 losses market inefficiencies (**Kickhöfer and Kern, 2015**). Usually, transportation users only  
120 account for marginal private costs, which may lead to welfare losses, since marginal social

121 costs are neglected. To overcome such issues, some authors have been proposed to  
122 internalize the difference between generalized prices and marginal social costs by a tool  
123 [e.g. **(Friesz et al., 2004; Small and Verhoef, 2007)**]. However, they focused only on  
124 congestion effects. Road vehicles also give rise to side effects such as the productivity  
125 losses due to lives lost in road crashes, health costs caused by air or the abatements costs  
126 due to climate impacts (**Bandeira et al., 2018a; Int Panis et al., 2004; Korzhenevych et**  
127 **al., 2014; Yeh, 2013)**.

128 Despite its relevance, the existing literature about the assessment of traffic externalities  
129 drawn on a common measure (e.g., sustainability indicator) is scarce (**Bandeira et al.,**  
130 **2014; El-Rashidy and Grant-Muller, 2015; Kickhöfer and Nagel, 2016; Sdoukopoulos**  
131 **et al., 2019; Torrao et al., 2016)** and mostly focused in urban areas (**Bandeira et al.,**  
132 **2018b; Sampaio et al., 2019; Tafidis et al., 2017; Yeh, 2013)**. **Torrao et al. (2016)**  
133 developed a safety, energy efficiency and green indicator based on crash consequences  
134 and type, and vehicle characteristics. The models neither accounted with impacts of  
135 changes in modal operation, nor included traffic volume as input. **Kickhöfer and Nagel**  
136 **(2016)** used an agent-based model to internalize air quality costs taking into account both  
137 traffic congestion and vehicle characteristics, but they focused only roads in urban areas.

138 Although rural roads represent 80% of the total road network length in developing countries  
139 (**Rivera et al., 2015)**, the development of link-based indicators reflecting traffic-related  
140 impacts for this type of roads is little explored. **El-Rashidy and Grant-Muller (2015)**  
141 introduced a fuzzy logic model for assessing the mobility of road transportation networks.  
142 The model incorporated a physical connectivity attribute and traffic condition as mobility  
143 attributes and was successful tested for different intercity routes. **Fernandes et al. (2018)**  
144 analyzed the impacts of partial-metering strategies at a rural corridor near a shopping mall  
145 to reduce emissions, noise and user perspective costs. The proposed system resulted in  
146 improvements (up to 13%) compared to the unmetered conditions. Recently, **Chang et al.**  
147 **(2018)** developed a road pricing model that integrated travel time, CO<sub>2</sub> emissions and safety

148 costs by combining them on a green safety indicator for evaluating the level of service in  
149 freeway traffic. However, the authors discarded impacts of local pollutants, such as PM.

150 Link-based indicators can be applied into advanced traffic management systems as vehicle  
151 routing problems, but existing literature around this topic is mostly focused on the use of  
152 empirical models for route choice optimization in urban areas (**Ćirović et al., 2014;**  
153 **Jovanović et al., 2014; Pamučar et al., 2016a; Pamucar and Goran Ćirović, 2018;**  
154 **Pamučar et al., 2016b**).

155 Thus, the following gaps in the literature review were revealed: *i)* none of the prior studies  
156 developed a sustainability indicator for integrating traffic externalities according to the road  
157 type, i.e., urban, rural and highway; *ii)* little is known about the impacts of site operational  
158 characteristics on each externality cost value; *iii)* few studies applied reliable methods for  
159 gathering the number of exposure people, who are directly affected to noise, NO<sub>x</sub> and PM.

160 The novelty of this research relies in the following aspects:

161

162 i) To use a simulation-based approach for quantifying and assessing external  
163 costs of road traffic at urban, rural and highway scales;

164 ii) To include a trade-off analysis among traffic externalities;

165 iii) To implement more effective eco-friendly and sustainable routing systems to  
166 include social, environmental and economic sustainable goals.

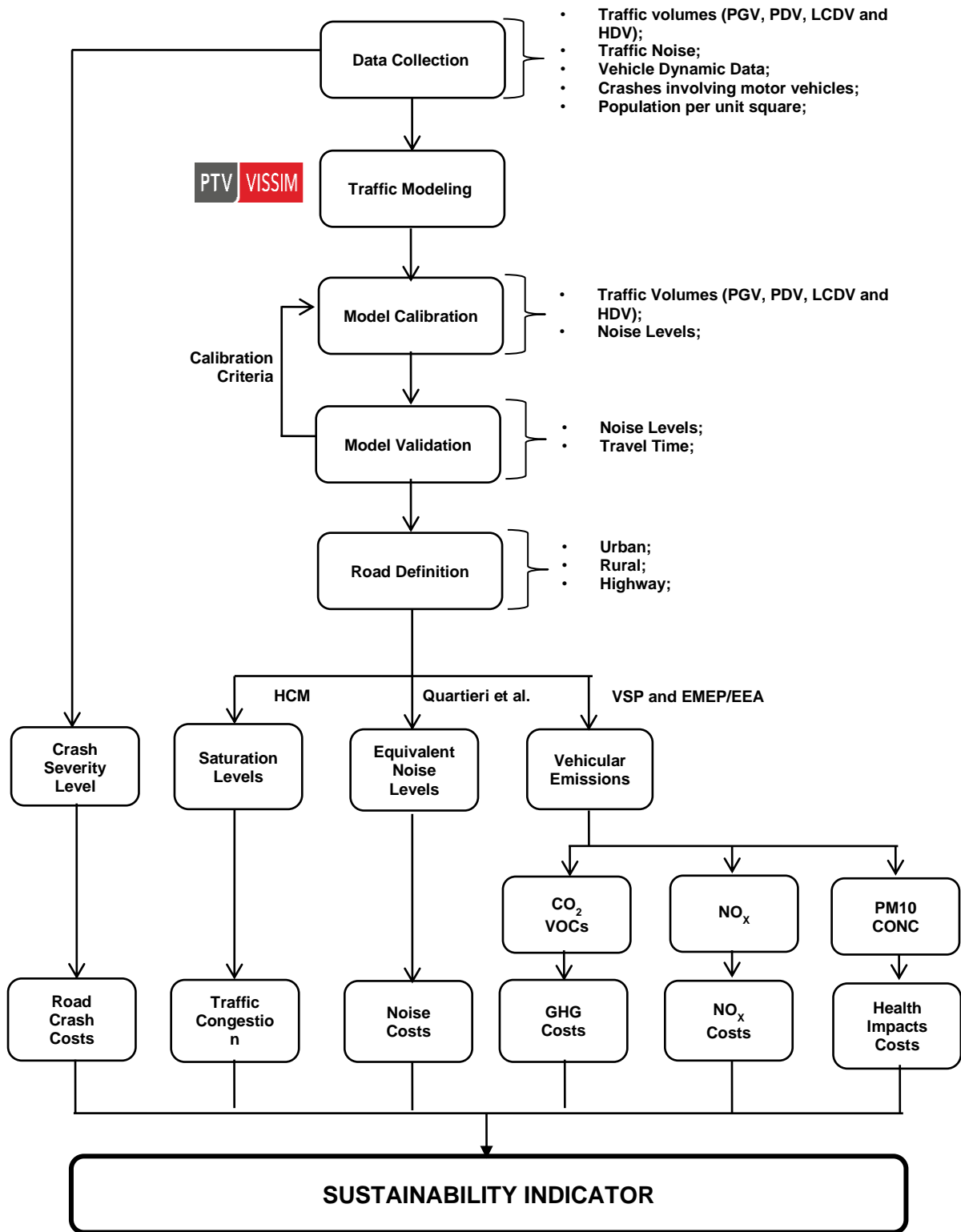
167

### 168 **3. METHODOLOGY**

169 The core idea of the methodology was to use and test a modeling platform to evaluate  
170 external costs of road transportation at a segment level. It proceeded in five steps,  
171 illustrated in Errore. L'origine riferimento non è stata trovata.. The development of the  
172 sustainability indicator involved first, collecting traffic volumes, noise, vehicle dynamic  
173 (second-by-second speed, acceleration and slope), crash data and population per unit

174 square from one real-world intercity corridor. Second, the modeling platform was calibrated  
175 and validated, and then, studied location was divided into multiple sub-segments according  
176 to the road type. Finally, external costs of road transportation (**Korzhenevych et al., 2014**)  
177 were computed to obtain the sustainability performance measure in monetary values.  
178





179

180 **FIGURE 1** Overview of the research methodology (PGV – Passenger Gasoline Vehicles,  
 181 PDV – Passenger Diesel Vehicles, LCDV – Light Commercial Diesel Vehicles; HDV –  
 182 Heavy Duty Vehicles; HCM – Highway Capacity Manual; VSP – Vehicle Specific Power;  
 183 EMEP/EEA – European Monitoring and Evaluation Programme by European  
 184 Environmental Agency; CONC – Concentrations).

185

### 186 3.1. Modeling Platform

#### 187 3.1.1. Road Traffic Modeling

188 VISSIM9.0 (PTV AG, 2016) (which stands for *Verkehr In Städten SIMulationsmodell*) was  
189 used to model road traffic operations, for four main reasons: 1) it allows setting several  
190 behavior parameters to reflect site-specific driving habits; 2) it accounts the variations in  
191 both vehicle speed and acceleration-deceleration profiles at rural and urban roundabouts  
192 and traffic lights, interchange ramps or conventional tolls (PTV AG, 2016); 3) it includes a  
193 calibration and validation of traffic-related metrics to set realistic representations of road  
194 traffic operations at urban (Fernandes et al., 2015), rural (Fernandes et al., 2018) and  
195 highway (Abou-Senna et al., 2013; Fontes et al., 2014; Fries et al., 2017) roads; 4) it  
196 exports vehicle dynamic and traffic volume (by vehicle type and segment-by-segment) data  
197 at high time resolutions that can be used by emission (Abou-Senna et al., 2013;  
198 Fernandes et al., 2015; Fontes et al., 2014), noise (Fernandes et al., 2018), and geo-  
199 processing tolls and air quality models (Borrego et al., 2016; Dias et al., 2018).

200

#### 201 3.1.2. Pollutant Emissions

202 CO<sub>2</sub> and NO<sub>x</sub> generated by Light Duty vehicles – LDV, i.e., PGV, PDV and LCDV were  
203 estimated using the VSP-based modeling approach that provides instantaneous vehicle  
204 power per unit mass (US EPA, 2002). This regression-based model is sensitive to changes  
205 in vehicle dynamic data and offers significant explanatory power for vehicle energy use and  
206 emissions rates IOVs (Hu et al., 2016). The use of VSP is justified because a speed-based  
207 approach as EMEP/EEA methodology, per se, is less robust to assess emissions of traffic  
208 singularities (roundabouts, traffic lights, toll plazas or stop-controlled intersections) and  
209 driving behavior states (acceleration, overtaking or gap acceptance) which in turn have  
210 impact on GHG and NO<sub>x</sub> external costs. VSP values are stratified into 14 bins, which in

211 turn correspond to an emission factor on a second-by-second basis (**US EPA, 2002**). VSP  
212 is a function of speed, acceleration-deceleration and slope, as shown in Equation 1 for LDV  
213 (**US EPA, 2002**):

214

$$215 \quad VSP = v \times [1.1a + 9.81 \sin(\arctan(\text{grade})) + 0.132] + 0.00302v^3, \quad (1)$$

216

217 where  $v$  is the instantaneous speed (m/s);  $a$  represents the instantaneous  
218 acceleration/deceleration ( $\text{m/s}^2$ ), and  $\text{grade}$  is the road slope (in decimal fraction).

219

220 Since VSP accounts for changes in vehicle dynamic with high resolution time, it shows as  
221 proper methodology for the quantification of exhaust emissions generated by PGV (**Anya**  
222 **et al., 2013**), PDV (**Coelho et al., 2009**), and LCDV (**Coelho et al., 2009**). A good body of  
223 literature has documented the effective use of VSP in assessing vehicular emissions in real-  
224 world urban, rural and highway routes (**Anya et al., 2013; Coelho et al., 2009; Khan and**  
225 **Frey, 2018**).

226 To obtain emissions estimates for HDV ( $\text{CO}_2$ ,  $\text{NO}_x$ , VOCs and PM) and LDV (PM and  
227 VOCs), the EMEP/EEA method was used (**EEA, 2013**). It uses emission factors for diesel  
228 HDV from Euro I to VI emission standards and engine capacities as a function of the  
229 average speed (**EEA, 2013**).

230 A GUI application in MATLAB was conceived and developed to compute second-by-second  
231 LDV and HDV dynamics data from VISSIM output (speed, acceleration and slope). LDV  
232 and HDV emissions were summed up and further assigned to a segment. Then, such  
233 information incorporated on a GIS platform to assess pollutant concentrations, as described  
234 in the following section.

235

### 236 3.1.3. Air Quality

237 The air quality at the urban scale were evaluated by applying the air quality modeling  
238 system URBan AIR (URBAIR) (**Borrego et al., 2014; Valente et al., 2014**). The URBAIR  
239 model is an improved version of the second generation Gaussian model POLARIS  
240 developed by **Borrego et al. (1997)**, differing from traditional Gaussian dispersion models  
241 in what concerns its dispersion parameters, which have a continuous variation with the  
242 atmospheric stability, and it accounts for building-induced dispersion mechanisms.

243 This steady state atmospheric dispersion model is based on boundary layer scaling  
244 parameters and is suitable to be used for distances up to about 10 km from the source. The  
245 URBAIR modelling system is designed to be modular and includes the pre-processing of  
246 land use and urban elements geometry (GIS-based), meteorological conditions and air  
247 pollutant emissions, coupled with a dispersion module. The system framework is designed  
248 in such a way that the inputs/outputs of the different modules are shared and linked along  
249 the modeling process.

250 The meteorological model calculates a set of meteorological parameters, such as  
251 atmospheric turbulence characteristics, mixing height, friction velocity, Monin-Obukhov  
252 length and surface heat flux, using as initial conditions, or measured data. Since the  
253 topography and build-up structure characteristics have a significant influence on the  
254 dispersion of atmospheric pollutants, particularly in urban areas, URBAIR also requires  
255 characterization of the spatial variation of terrain surface elevation, buildings 3D  
256 coordinates and roads 2D coordinates. For simplicity, buildings can be assembled based  
257 on proximity and geometry criteria.

258 URBAIR considers different types of source emissions, namely, area, volume, point (such  
259 as industrial facilities and combustion activities for residential and services sectors) and line  
260 sources (road traffic emissions). As outputs, URBAIR provides air quality patterns for a  
261 given spatial domain (with up to about 50 km from the domain center) and time period (e.g.,

262 hourly, daily, one year or multiple years) for different air pollutants, namely: PM10, Nitrogen  
 263 dioxide (NO<sub>2</sub>), Sulfur dioxide (SO<sub>2</sub>) and CO.

264 URBAIR model has been widely applied and extensively tested, having showed capability  
 265 to produce robust and realistic results. Recent works showed its usefulness and capability  
 266 to perform air quality studies at urban scale (**Borrego et al., 2016; Dias et al., 2018**).

267 In this study, URBAIR model was selected for two main reasons: 1) it is designed to assess  
 268 the impact of urban planning and traffic management on air quality; 2) it is an advanced  
 269 Gaussian model that has been enhanced with several major features, mainly the treatment  
 270 of road traffic emissions and 3D urban elements.

271

#### 272 3.1.4. Noise

273 The prediction of noise levels was made using a numerical approach developed by  
 274 **Quartieri et al. (2010)**. This procedure relates directly the acoustical energy sent to a  
 275 receiver to the number of vehicles, to the source-receiver distance and to the mean traffic  
 276 speed. The above information is used to assess source power levels and then, equivalent  
 277 noise levels for a particular segment  $k$  ( $L_{eq,k}$ ), which are obtained at a fixed distance  $d$ ,  
 278 according to the distance between the road axis and the receiver. Equation 2 gives the  
 279 hourly equivalent noise level by segment (**Guarnaccia, 2013**):

280

$$281 \quad L_{eq,k} = 10 \log(V_{LDV} + nV_{HDV}) + 53.6 + 26.8 \log v_k - 20 \log d - 46.563, \quad (2)$$

282

283 where  $L_{eq,k}$  is the segment-specific equivalent noise level (dBA);  $V_{LDV}$  and  $V_{HDV}$  are the  
 284 hourly LDV and HDV, respectively, volumes (vph);  $n$  represents the acoustic equivalent,  
 285 i.e., the number of LDV that produce the same noise of a HDV;  $v_k$  is the segment-specific

286 average speed ( $\text{km}\cdot\text{h}^{-1}$ );  $d$  – Distance between the road axis and the receiver (m) (**Quartieri**  
287 **et al., 2010**).

288 The advantage of this type of semi dynamic noise model is that only information about  
289 vehicle speed and traffic volumes for a given segment is needed. This means that one do  
290 not take into account a new equation for noise for every other region or country.

291 To obtain day-evening-night level ( $L_{den,k}$ ) on a segment  $k$  (dBA), the hourly segment-specific  
292 equivalent level ( $L_{eq,k}$ ) was assumed to be the same during all day. This is a conservative  
293 assumption since during the night traffic noise is usually lower than during daytime (**EEA,**  
294 **2018b**). Thus,  $L_{den}$  was computed using Equation 3:

295

$$296 \quad L_{den,k} = 10 \log \left[ \frac{1}{24} \left( 12 \cdot 10^{\frac{L_{eq,k}}{10}} + 4 \cdot 10^{\frac{L_{eq,k}+5}{10}} + 8 \cdot 10^{\frac{L_{eq,k}+10}{10}} \right) \right] \quad (3)$$

297

### 298 3.1.5. Calibration and Validation

299 The modeling platform was calibrated and validated using field data collected from the  
300 studied location. The data were divided in training (70%) and testing (30%) sets (**Liu et al.,**  
301 **2017**), randomly selected before calibration procedure. The following strategy was used:

302

- 303 • Capacity Calibration – Simulated and observed traffic volumes were compared for  
304 each monitoring point. The stopping criterion for this step was: at least 85% must  
305 meet the criteria of GEH (acronym for Geoffrey E. Havers) < 4 (**Yu and Fan, 2017**);
- 306 • Route Choice and Noise Calibration – Simulated travel time per each route as well  
307 as noise were compared against the training data. The procedure stops when the  
308 difference in sample mean was not statistically significant within a 95% confidence  
309 level ( $p\text{-value} < 0.05$ );

- 310 • Route Choice and Noise Validation – Site-specific simulated and testing set of travel  
311 time and noise were compared with 10 random seed runs (Winnie et al., 2014).

312

### 313 3.2. Sustainability Indicator

314 The proposed sustainability indicator is intended to account monetary costs per vehicle  
315 ( $\text{€} \cdot \text{veh}^{-1}$ ) from road transportation activities in terms of: 1) congestion; 2) noise; 3) GHG; 4)  
316  $\text{NO}_x$ ; 5) health impacts; and 6) road crashes. The following paragraphs describe in detail  
317 each cost component calculations.

318

#### 319 3.2.1. Traffic Congestion

320 For a given segment, depending on the road type, congestion level is represented by the  
321 volume-to-capacity ratio defined as  $V/C$ , where the volume  $V$  is the mixed traffic (expressed  
322 in passenger car units per hour –  $\text{pcu} \cdot \text{h}^{-1}$  per lane length) which takes into account HDV  
323 adjustment factors as suggested by the Highway Capacity Manual Sixth Edition (HCM,  
324 2016), and the capacity  $C$  is the theoretical maximum traffic volume along segment which  
325 is estimated according to the type of facility (HCM, 2016), as follows:

326

327 Urban and Rural Segments – 1 600  $\text{pcu} \cdot \text{h}^{-1}$  per lane;

328 Highway Segments – 2 500  $\text{pcu} \cdot \text{h}^{-1}$  per lane;

329 Weaving, On-ramp, Off-ramp and Basic Segments – 2 200  $\text{pcu} \cdot \text{h}^{-1}$  per lane (HCM, 2016).

330

331 Each segment-specific  $V/C$  ratio results in five congestion levels, as follows  
332 (Korzhenevych et al., 2014): 1 (free-flow) –  $V/C < 0.25$ ; 2 – if  $0.25 < V/C < 0.50$ ; 3 –  $0.50$   
333  $< V/C < 0.75$ ; 4 (near capacity) –  $0.75 < V/C < 1$ ; 5 (over capacity)  $V/C > 1$ . Each level is  
334 then, associated to a congestion cost ( $CC_k$ ) on a segment that can be adjusted to the local

335 conditions, road type and vehicle type (Korzhenevych et al., 2014), as given by Equations  
336 4 to 7:

337

$$338 \quad TC_k = \frac{c_{LDV} V_{LDV} + c_{HDV} V_{HDV}}{V_{LDV} + V_{HDV}} I_k, \quad (4)$$

$$339 \quad c_{LDV} = f\left(\frac{V}{C}\right), \quad (5)$$

$$340 \quad c_{HDV} = f\left(\frac{V}{C}\right), \quad (6)$$

$$341 \quad L_i = f\left(\frac{V}{C}\right), \quad (7)$$

342

343 where  $TC_k$  is the traffic congestion cost on a segment  $k$  (€·veh<sup>-1</sup>);  $c_{LDV}$  and  $c_{HDV}$  are the local  
344 congestion costs for LDV and HDV, respectively, depending on the  $V/C$  according to the  
345 type of road (urban, rural and highway) (€/veh.km);  $I_k$  is the length of the segment  $k$  (km);  
346 and  $L_i$  is the level of congestion, which also depends on the  $V/C$  ( $i = 1, \dots, 5$ ).

347

### 348 3.2.2. Noise

349 The approach for estimating segment-specific noise costs is based on the cost of noise in  
350 €/dBA per exposed person and per hour of the local population potentially exposed to a  
351 certain noise range considering the LDV and HDV traffic in kilometers traveled, as given by  
352 Equation 8:

353

$$354 \quad N_k = \frac{CL_{den, k} pop_k}{ab(V_{LDV} + V_{HDV}) I_k}, \quad (8)$$

355



356 where  $N_k$  is the noise cost on a segment  $k$  (€·veh<sup>-1</sup>);  $CL_{den, k}$  is the cost of a given day-  
 357 evening-night noise level  $L_{den, k}$  (€/dBA per person and per year) adjusted to the local  
 358 conditions and type of road (Korzhenevych et al., 2014);  $pop_k$  is the number of individuals  
 359 potentially exposed to the noise level  $L_{den, k}$  (inhabitants per km of segment length) that is  
 360 represented by local population; and  $a$  and  $b$  are equal to 365 (number of days) and 24  
 361 (number of hours), respectively.

362

### 363 3.2.3. GHG

364 In this paper, CO<sub>2</sub> and VOCs emissions were considered for the cost quantification related  
 365 with the impact of GHG on environment, human health and economy. The cost estimation  
 366 procedure involved three steps: 1) to compute emissions to the overall network according  
 367 to the share of LDV and HDV; 2) to assign emissions to a segment; 3) to calculate segment-  
 368 specific emission costs based in the costs provided in using Equation 9:

369

$$370 \quad GHG_k = \alpha_1 \left( \frac{\sum_{j=1}^5 \sum_{i=1}^{N_k} v_j ef_{CO_2, j, i, k}}{V_{LDV}} + \frac{E_{CO_2, HDV, k}}{V_{HDV}} \right) + \alpha_2 \left( \frac{E_{VOCs, LDV, k}}{V_{LDV}} + \frac{E_{VOCs, HDV, k}}{V_{HDV}} \right), \quad (9)$$

371

372 where  $GHG_k$  is the GHG cost on a segment  $k$  (€·veh<sup>-1</sup>);  $\alpha_1$  is the local damage cost of CO<sub>2</sub>  
 373 (Korzhenevych et al., 2014) (€·g<sup>-1</sup>);  $v_j$  is the share of the vehicle type  $j$  in the LDV vehicle  
 374 park fleet;  $ef_{CO_2, j, i, k}$  is the CO<sub>2</sub> emission factor vehicle type  $j$  in the second of travel  $i$  on  
 375 segment  $k$  (g·s<sup>-1</sup>);  $E_{CO_2, HDV, k}$  represents the HDV CO<sub>2</sub> emissions on a segment  $k$  (g·s<sup>-1</sup>);  $N_k$   
 376 is the travel time on segment  $k$  (s);  $\alpha_2$  is the local damage cost of VOCs (Korzhenevych  
 377 et al., 2014) (€·g<sup>-1</sup>);  $E_{VOCs, LDV, k}$  represents the LDV VOCs emissions on a segment  $k$  (g·s<sup>-1</sup>)  
 378 1); and  $E_{VOCs, HDV, k}$  represents the HDV VOCs emissions on a segment  $k$  (g·s<sup>-1</sup>).

379

### 380 3.2.4. NO<sub>x</sub>

381 The quantification of NO<sub>x</sub> costs accounts for the impacts on local population which is  
 382 represented by the ratio between segment population and national population densities, as  
 383 given by Equation 10:

384

$$385 \quad NO_{Xk} = \beta \frac{D_k}{D_N} \left( \frac{\sum_{j=1}^5 \sum_{i=1}^{N_k} v_j ef_{NO_x, j, i, k}}{V_{LDV}} + \frac{E_{NO_x, HDV, k}}{V_{HDV}} \right), \quad (10)$$

386

387 where  $NO_{Xk}$  is the NO<sub>x</sub> cost on a segment  $k$  (€·veh<sup>-1</sup>);  $\beta$  is the local damage cost of NO<sub>x</sub>  
 388 (Korzhenevych et al., 2014) (€·g<sup>-1</sup>);  $D_k$  is the number of individuals for segment  $k$  per  
 389 square kilometer;  $D_N$  is the national population density;  $ef_{NO_x, j, i, k}$  is the NO<sub>x</sub> emission factor  
 390 vehicle type  $j$  in the second of travel  $i$  on segment  $k$  (g·s<sup>-1</sup>); and  $E_{NO_x, HDV, k}$  represents the  
 391 HDV NO<sub>x</sub> emissions on a segment  $k$  (g·s<sup>-1</sup>).

392

### 393 3.2.5. Health Impacts

394 Currently, it is well known that air pollution, mainly by the form of particles with an  
 395 aerodynamic diameter smaller than 10 μm (PM10), is an important incentive for the  
 396 development and exacerbation of respiratory diseases, such as asthma, chronic obstructive  
 397 pulmonary disease or lung cancer, as well as a substantial impact on cardiovascular  
 398 disease (Costa et al., 2014; R uckerl et al., 2011).

399 The evaluation of the health cost linked to the health impacts can be performed by  
 400 multiplying the Years of Life Lost (YOLL) value by its associated economic value.  
 401 Vlachokostas et al. (2012) suggest the average value of 52 000€ by YOLL. Based on the  
 402 achieved air quality state for a specific situation, the health impact cost on a segment  $k$ ,  
 403 related with PM10 on an hourly basis may be computed using Equation 11:

404

$$405 \quad HI_k = 52\,000 \frac{CFR \, pop_{30k} \, c_k}{ab(V_{LDV} + V_{HDV})}, \quad (11)$$

406

407 where  $HI_k$  represents the health impacts cost on a segment  $k$  (€·veh<sup>-1</sup>);  $CFR$  is the  
 408 correlation coefficient between the PM10 concentration variation and the probability of  
 409 experiencing or avoiding a specific health indicator, which was set to 0.0004  
 410 YOLL/(person·year·µg·m<sup>-3</sup>) (EC, 2006);  $pop_{30,k}$  is the number of individuals potentially  
 411 exposed over 30 years (inhabitants per km of segment length); and  $c_k$  is the average PM10  
 412 concentration on a segment  $k$  (µg·m<sup>-3</sup>).

413

#### 414 3.2.6. Road Crashes

415 The level of external crash costs depends not only on the crash severity, but also on the  
 416 insurance system, i.e., social costs of traffic-related crashes (Korzhenevych et al., 2014).  
 417 These costs can be obtained by applying an adjusted risk that involves the following cost  
 418 components: *i*) death and injury due to an accident for the person exposed to risk; *ii*) for the  
 419 relatives and friends of the person exposed to risk; and *iii*) crash cost for the rest of the  
 420 society. These considerations are summarized in Equation 12:

421

$$422 \quad RC_k = \frac{X_F SC_F + X_{SI} SC_{SI} + X_{LI} SC_{LI}}{ab(V_{LDV} + V_{HDV}) I_k}, \quad (12)$$

423

424 where  $RC_k$  is the road crash cost on a segment  $k$  (€·veh<sup>-1</sup>);  $X_F$ ,  $X_{SI}$ ,  $X_{LI}$  are the annual  
 425 numbers of fatalities, serious and light injury cases, respectively, on a segment  $k$ ; and  $SC_F$ ,  
 426  $SC_{SI}$ ,  $SC_{LI}$  represent the average social accident costs (€) for crashes involving fatalities,  
 427 serious and light injuries, respectively, adjusted to local conditions.

428

429 **3.2.7. External Cost by segment and by route**

430 The total external cost on a segment  $k$  is defined as the sum of the above cost components  
 431 for a segment, and denoted as  $EC_k$  (€·veh<sup>-1</sup>), as expressed by Equation 13:

432

$$433 \quad EC_k = TC_k + N_k + GHG_k + NO_{xk} + HI_k + RC_k. \quad (13)$$

434

435 Lastly, the external cost associated to a route  $r$  for a specific travelling direction, here  
 436 denoted by  $EC_r$  (€·veh<sup>-1</sup>), is the sum of costs for all segments  $k \in M_r$ , where  $M_r$  is the set of  
 437 segments along the route  $r$ , along that path, as given in Equation 14:

438

$$439 \quad EC_r = \sum_{k \in M_r} EC_k. \quad (14)$$

440

441 **4. CASE STUDY**

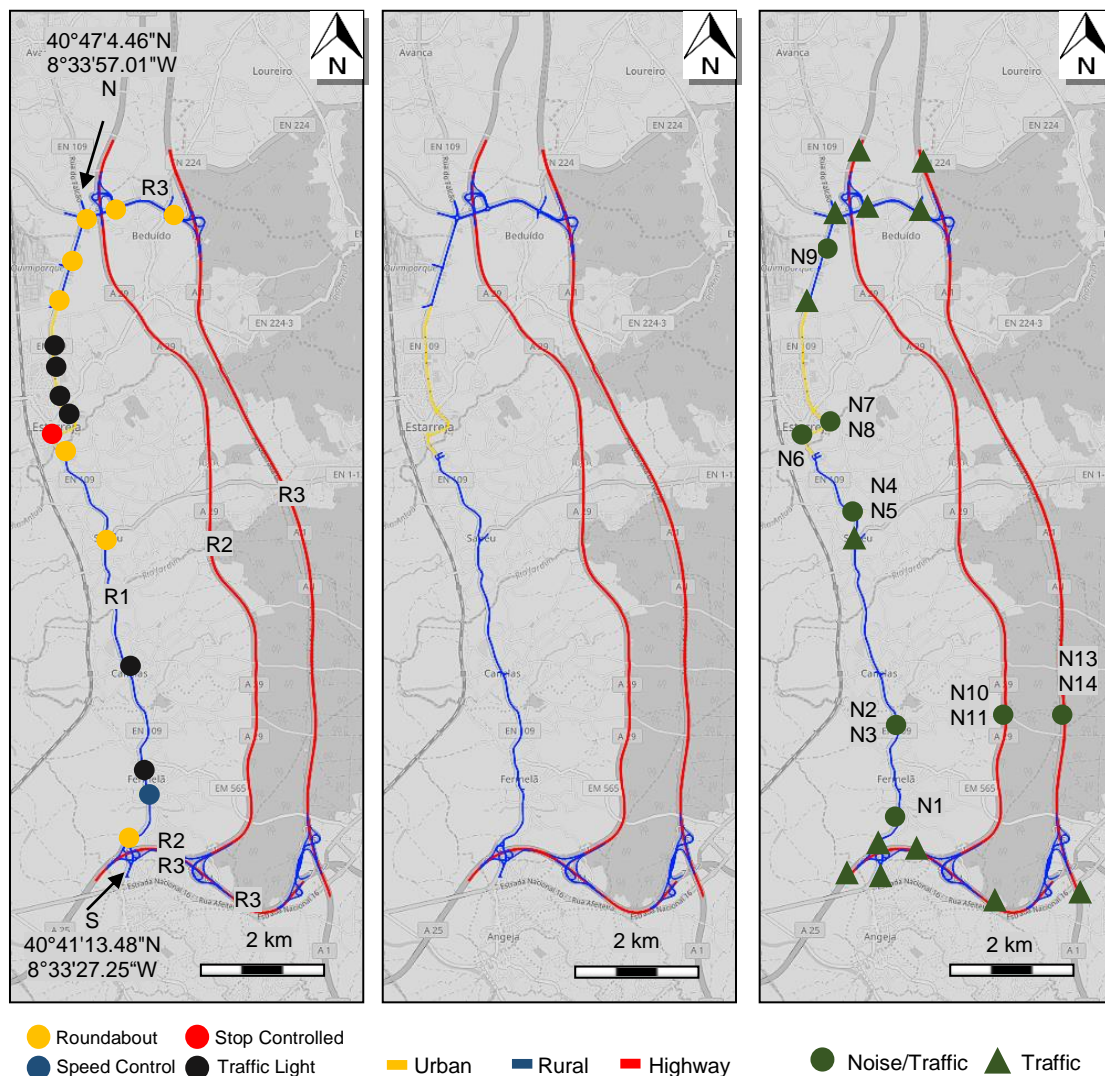
442 An origin-destination (South to North; North to South) pair, comprising three parallel  
 443 alternative routes, was sought out for this research. Prior research carried out in this area  
 444 have shown that road type has impact on pollutant emissions (**Bandeira et al., 2013**). This  
 445 intercity corridor provides a direct connection between Aveiro and Estarreja (Portugal) and  
 446 is near a high-density industrial complex with moderate HDV traffic; hence, the air quality  
 447 and traffic-related noise can represent an important issue, especially for local population.

448 **Errore. L'origine riferimento non è stata trovata.**-a shows the candidate location with routes  
 449 identification (R1-R2-R3). These routes were chosen based on their different specificities.

450 The routes include urban (with speed ( $s$ ) limits in the range  $0 \leq s \leq 50$  km/h), rural ( $50 \leq s \leq 90$   
 451 km/h) and highway ( $90 \leq s \leq 120$  km/h) trip sections (**Errore. L'origine riferimento non è**  
 452 **stata trovata.**-b). R1 is partly conducted on a rural (63%) and urban (37%) roads, while R2

453 is mostly a low-traffic-volume section (75%) traversing A29 highway, which has 2 lanes on  
 454 each direction and an electronic pay toll system. Approximately 65% of R3 is on a high-  
 455 traffic-volume section along A1 highway, with 2 lanes on each direction, and it includes both  
 456 conventional and electronic pay toll systems. Average daily traffic (ADT) on A1 and A29  
 457 study segments is about 39 950 and 11 700, respectively (IMT, 2019). It must be noted that  
 458 the classification of roads was based on posted speed limits and also on population density  
 459 (Korzhenevych et al., 2014).

460



461

462

463

**FIGURE 2** Study Domain: a) Routes Aerial View; b) Type of Road; c) Data Monitoring Points. Background Map Source [Open Street Maps].

464

465

466 **4.1. Data collection**

467 Traffic data were collected in morning (7:00AM-10AM), off-peak (11AM-2PM) and evening  
468 peak (5PM-7PM) during six typical weekdays in May and June 2018 under dry and windless  
469 weather. Traffic volume manual counting was performed in 15-min time intervals (in both  
470 travelling directions) at specific sites and video cameras were used to collect intersection-  
471 specific demand and turning split distributions. ADT volumes for A1 and A29 highways were  
472 retrieved from the Institute for Mobility and Transport (IMT, 2019), and complemented with  
473 the available images of video cameras installed at the top of highway bridges. A total of 42  
474 monitoring points (including intersection entry and exit points) were evaluated in the studied  
475 location, allowing an accurate assignment of road traffic along the overall network.

476 Sound pressure levels were measured using an integrating sound level meter RION-NL52  
477 (0.1-s basis) installed in 14 locations points of the study network, as depicted in Errore.  
478 L'origine riferimento non è stata trovata.-c. To account for variability in noise values, tests  
479 were conducted in cruise speed (N2/N3), acceleration (N1/N4/N6/N9) and highway (bridges  
480 – N10/N11/N13/N14; wayside – N12) points. The microphone was in the acoustic field at  
481 1.5 m from the ground (height of tripod) and at 7.5 m and 15 m from the main road axis in  
482 R1 and R2-R3, respectively. More than 50 data sets of 15-min (equivalent continuous  
483 sound level –  $L_{eq}$  and respective arterial traffic) were collected.

484 Six routes across the study domain were covered using GNSS data-logger and On-Board  
485 Diagnostic (OBD-II) system in nine equipped LDV (gasoline and diesel) and six different  
486 drivers to record vehicle speed in 1-s interval. These routes are defined as follows: *i*) North  
487 to South (R1); *ii*) South to North (R1); *iii*) North to South (R2); *iv*) South to North (R2); *v*)  
488 North to South (R3); *vi*) South to North (R3). Prior to on-road dynamic tests, the minimum  
489 number of travel time trips was determined for each route. Thus, taking into account the

490 ADT observed in R2 [vehicles per lane <15 000 (**IMT, 2019**)] and R3 [15 000<vehicles per  
491 lane<20 000 (**IMT, 2019**)] and traffic signal density (<3TL/1.6 km) in R1, the minimum  
492 sample size is 8 (**Turner, 1998**). Almost 1 300 km of road coverage data over the course  
493 of 22h were collected (90 GNSS travel time trips – 15 per route).

494 Air quality within the study area was estimated for a simulation domain defined over the  
495 road traffic network, with dimensions of 13 x 16 km<sup>2</sup>, as shown in **Errore. L'origine**  
496 **riferimento non è stata trovata.-b**. Since the road traffic emissions have been calculated  
497 with a high level of detail, a mesh resolution of 20 x 20 m<sup>2</sup> have been used (in a total of 717  
498 213 cells). Road traffic emissions were estimated following the methodology described in  
499 **Section 3.1.2**. The contribution of industrial areas and point sources inside the domain  
500 (e.g., some bakeries using wood burning ovens or residential combustion), were accounted  
501 as suburban background. The URBAIR domain covers the densely urbanized areas near  
502 the road network (located in a radius of 5 km from the highway road) allowing for the  
503 calculation of the health impacts. According to the methodology described in **Section 3.2.5**,  
504 the simulations were carried out for PM10.

505 Crash data involving motor vehicles along R1, R2 and R3 were gathered for 3-years' time  
506 period between 2015 and 2017 (**ANSR, 2017**). This period was selected for two main  
507 reasons: 1) A29 highway had no tolls until September 2010. After tolls introduction, the  
508 segment traffic dropped more than half (**IMT, 2011**); 2) lack of precise GPS coordinates  
509 before 2015 in order to assign to a specific segment. For the purpose of this study, crashes  
510 involving motor vehicles involving injuries and/or fatalities were selected and georeferenced  
511 on ArcGIS 10.5.0.6491 (**ERSI, 2016**). The database covered a total of 68 crash  
512 observations.

513

#### 514 4.2. Case Study Coding

515 Posted speed limits along the study domain and gap acceptance (critical and follow-up  
516 headways) in roundabout approaches were considered taking into account local driving  
517 habits (**Vasconcelos et al., 2013**). The dwell time distribution at conventional pay tolls was  
518 assumed to be same for all gates (6.8-9.6 s) (**Coelho et al., 2005**). The simulation runs  
519 lasted 90 minutes with a 30-min warm-up period to load traffic onto the road network. The  
520 simulation network in VISSIM is exhibited in *Errore. L'origine riferimento non è stata*  
521 *trovata..*

522 CO<sub>2</sub> and NO<sub>x</sub> emission rates for LDV were based on a local car fleet (**EMISIA, 2017**): 39%  
523 (1.4L: 33%, 1.8L: 5.95%, 2.2L: 0.05%) LDGV, 40% LDDV (1.9L), and 21% LDDT (2.5L).  
524 Since the terrain is flat in the study area, the effect of slope (Equation 1) was ignored.  
525 Concerning the EMEP/EEA methodology, the least squares fitting technique was used to  
526 find the data best-fitting curve to relate segment-specific average speed and emissions  
527 generated by local HDV and LDV taking into account the above car fleet composition  
528 (**EMISIA, 2017**) and considering representatives vehicles and their emission standards, the  
529 annual activity (vehicle kilometers traveled per year), and engine size and capacity of the  
530 vehicle. Bus activity was also ignored since it represented less than 1% of corridor-specific  
531 traffic.

532

#### 533 4.3. Segments Definition

534 The study domain was divided into multiple segments to compute each cost component  
535 and associated external cost by route. This level of segmentation was motivated by  
536 differences in type of road, downstream traffic control treatment, traffic volumes, number of

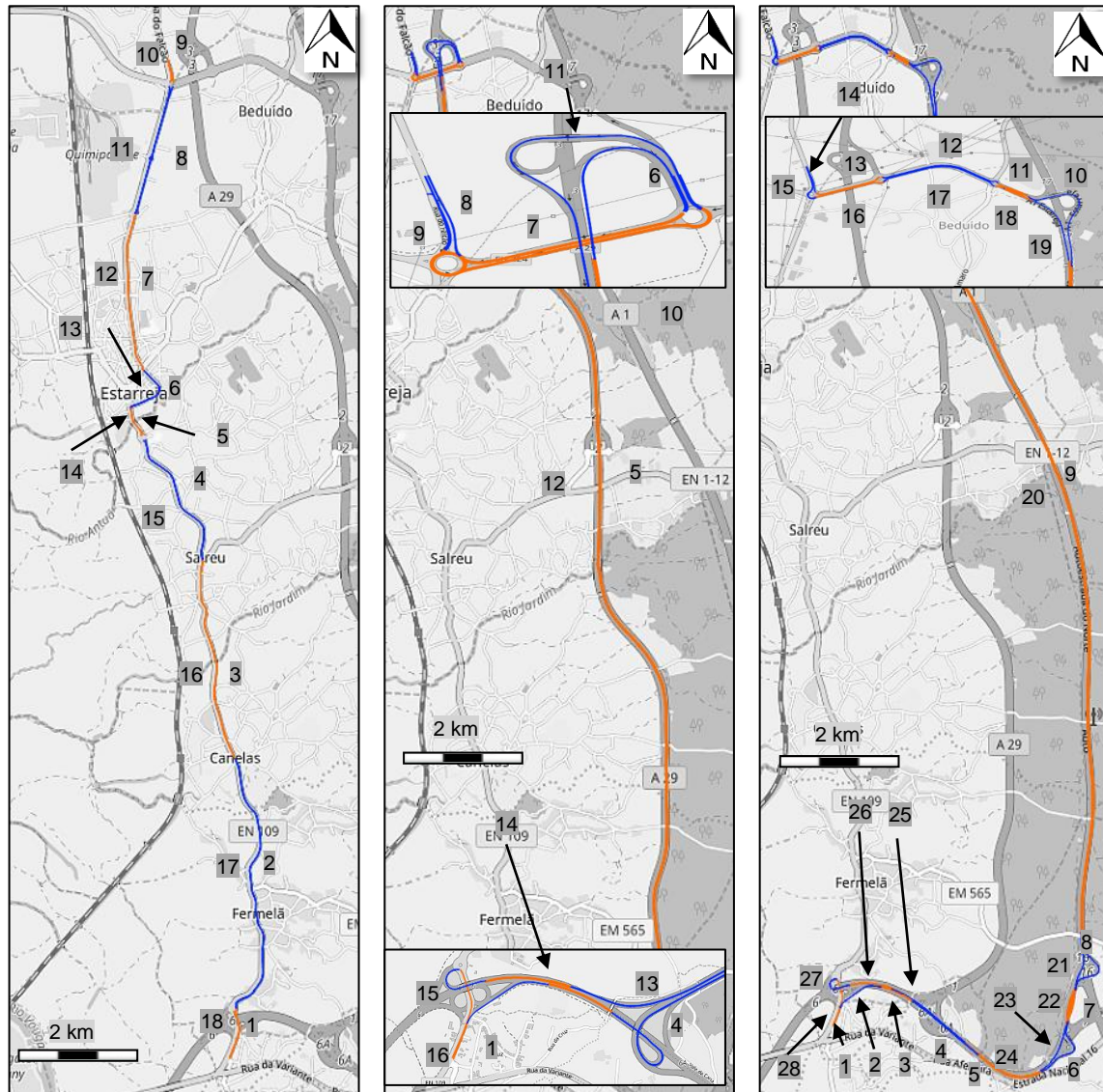


537 crashes and number of lanes. The proposed segmentation is exhibited in

a)

b)

c)



538

539 a-c and includes each travelling direction. To account the number of individuals potentially

540 exposed ( $pop_k$ ), the population density per square kilometer along the study domain

541 (**Statistics of Portugal, 2018**) was used. For the purpose of the analysis,  $pop_k$  was

542 computed based on the percent of segment within each square in **Errore**. L'origine

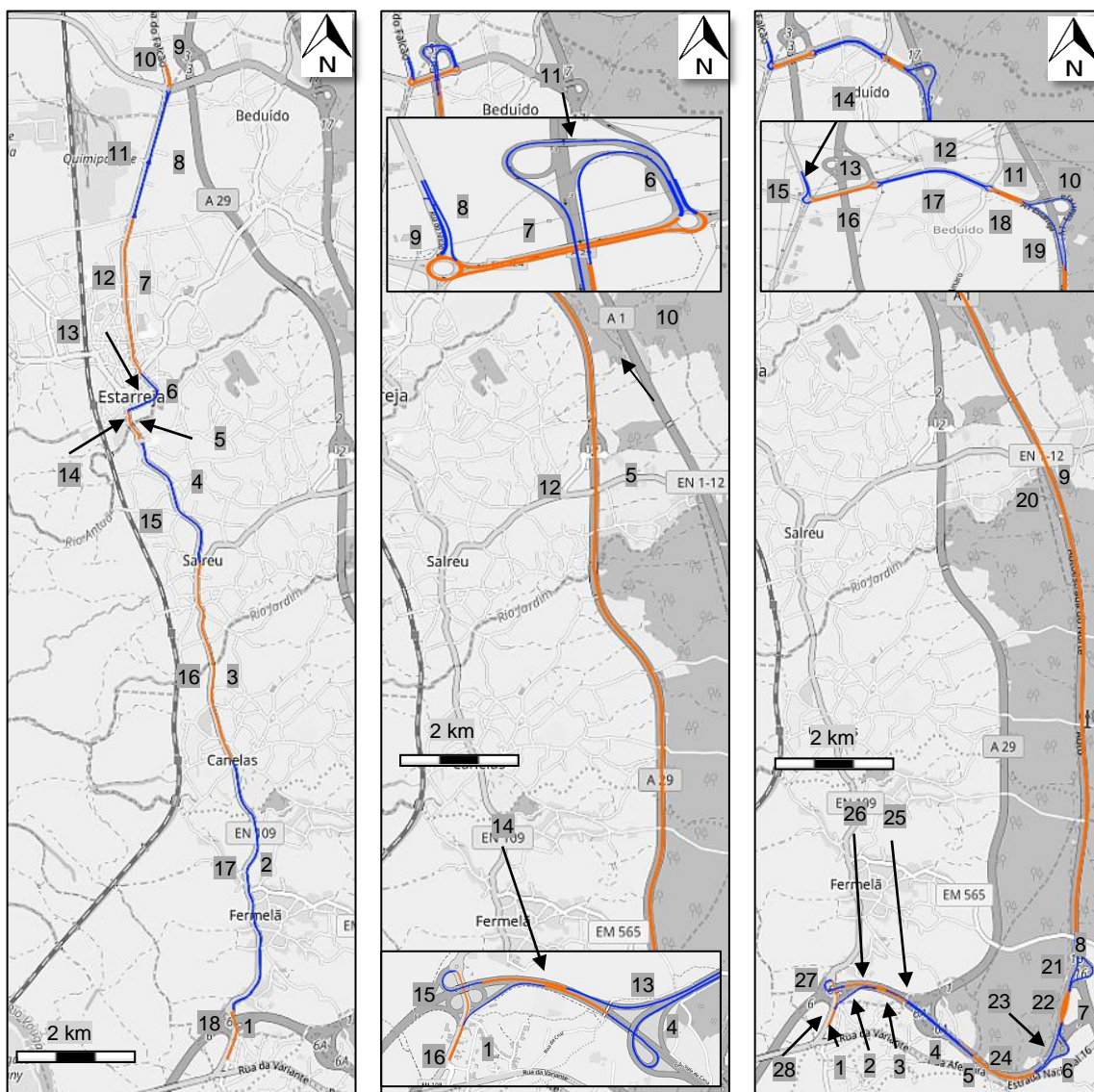
543 riferimento non è stata trovata.. **Errore. L'origine riferimento non è stata trovata.**

544 describes segment-specific information, including corresponding route and type of road.

a)

b)

c)



545

546 **FIGURE 3** Segments definition by route: a) R1; b) R2; c) R3. Background Map Source  
 547 [Open Street Maps].

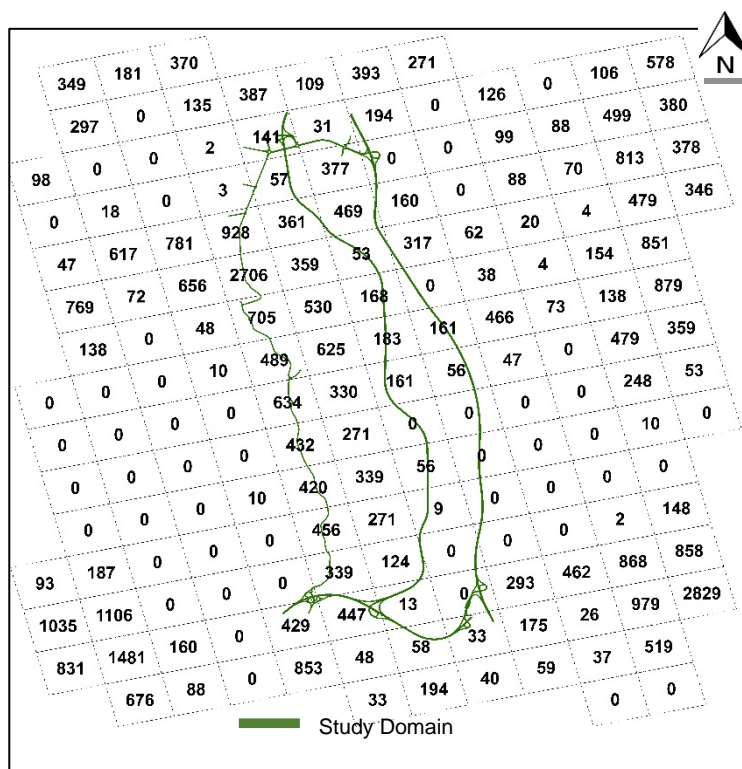
548

549

**TABLE 1** Key characteristics of proposed segments

Route	South-North			North-South		
	Segment ID	Type of Road	Length <sup>a</sup> [km]	Segment ID	Type of Road	Length <sup>a</sup> [km]
R1	1	Rural	0.56	10	Rural	0.33
	2	Rural	2.97	11	Rural	1.45
	3	Rural	2.23	12	Urban	1.72
	4	Rural	1.59	13	Urban	0.69
	5	Urban	0.35	14	Urban	0.34
	6	Urban	0.69	15	Rural	1.59
	7	Urban	1.73	16	Rural	2.23
	8	Rural	1.51	17	Rural	2.97
	9	Rural	0.26	18	Rural	0.53
R2	1	Rural	0.22	9	Rural	0.33
	2	Rural	0.56	10	Rural	0.49
	3	Highway	0.41	11	Rural	1.03
	4	Rural	1.49	12	Highway	10.90
	5	Highway	11.00	13	Rural	1.06
	6	Rural	0.64	14	Highway	0.50
	7	Rural	0.47	15	Rural	0.38
	8	Rural	0.26	16	Rural	0.53
R3	1	Rural	0.22	15	Rural	0.33
	2	Rural	0.56	16	Rural	0.49
	3	Highway	0.41	17	Rural	1.03
	4	Highway	0.96	18	Rural	0.86
	5	Highway	0.83	19	Rural	0.66
	6	Rural	0.85	20	Highway	9.49
	7	Rural	0.99	21	Rural	0.60
	8	Rural	0.75	22	Rural	0.89
	9	Highway	9.48	23	Rural	0.58
	10	Rural	1.10	24	Highway	1.04
	11	Rural	0.56	25	Highway	1.03
	12	Rural	0.89	26	Highway	0.50
	13	Rural	0.47	27	Rural	0.38
	14	Rural	0.26	28	Rural	0.53

550 *Note – a) Length by direction*



551

552 **FIGURE 4** Local population density per square kilometer (**Statistics of Portugal, 2018**).

553 Source [ArcGIS].

554

555 **4.4. Marginal cost factors**556 The marginal cost factors for the proposed sustainability indicator defined in **Section 3.2**557 are presented in **TABLE 1** and **TABLE 2** for congestion and noise components,

558 respectively, according to the site-specific conditions. These values, provided in

559 **Korzhenevych et al. (2014)**, are used to express transportation externalities into monetary

560 terms for road trip sections in Portugal (year 2010). Concerning the emissions and road

561 crashes, the following values were adopted (**Korzhenevych et al., 2014**):  $c_1 = 9 \times 10^{-5} \text{ €} \cdot \text{g}^{-1}$ 562  $^1$ ;  $c_2 = 1\,048 \times 10^{-6} \text{ €} \cdot \text{g}^{-1}$ ;  $c_3 = 1\,957 \times 10^{-6} \text{ €} \cdot \text{g}^{-1}$ ;  $SC_F = 1\,505\,000 \text{ €}$ ;  $SC_{SI} = 210\,000 \text{ €}$ ; and563  $SC_{SI} = 13\,800 \text{ €}$ . The population density ( $D_N$ ) was 112 inhabitants per kilometer square564 (**Statistics of Portugal, 2018**).

565

566 **TABLE 1** Marginal cost factors for congestion according to the type of road  
 567 (Korzhenevych et al., 2014).

Parameter	V/C	$L_i$	Urban (€/vkm)	Rural (€/vkm)	Highway (€/vkm)
$C_{LDV}$	0	1	0.0	0.0	0.0
	0.25	2	0.0	0.0	0.0
	0.5	3	0.0	0.0	0.0
	0.75	4	3.8	1.4	1.0
	1	5	5.9	4.7	2.4
$C_{HDV}$	0	1	0.1	0.1	0.0
	0.25	2	0.1	0.1	0.0
	0.5	3	0.1	0.1	0.0
	0.75	4	7.2	2.7	2.0
	1	5	11.2	9.0	4.6

568

569 **TABLE 2** Marginal cost factors for noise exposure (Korzhenevych et al., 2014).

$L_{den, k}$ (dBA)	$CL_{den, k}$ (€/dBA per person and per year)
51	6
55	29
60	56
65	84
70	113
75	187

*Note – Values within threshold intervals are computed using linear interpolation*

570

## 571 5. RESULTS AND DISCUSSION

572 In this section, the main results from the field data are analyzed (Section 5.1) followed by  
 573 the calibration and validation of the modeling platform (Section 5.2), and finally, a  
 574 representation of the external costs for the studied location is presented (Section 5.3).

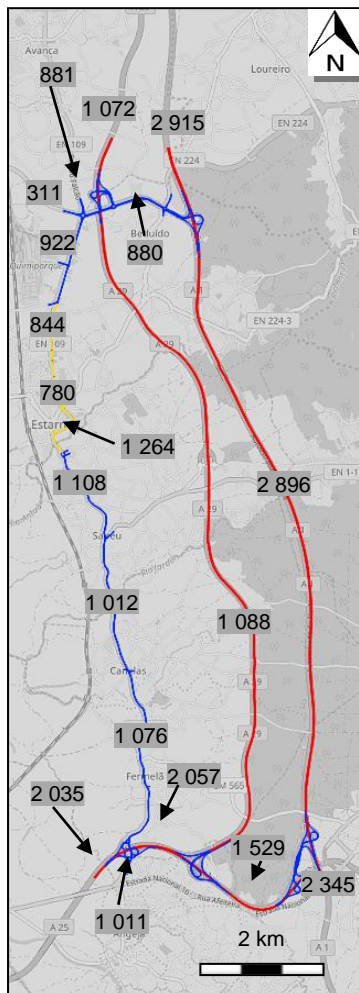
575

### 576 5.1. Field Data

577 The analysis of field data suggested the peak hour occurred between 5:30-6:30PM. Thus,  
 578 such period was selected for the assessment of road transportation external costs.



579 The hourly traffic volumes distribution (both travelling directions) along the study domain is  
 580 shown in **Errore. L'origine riferimento non è stata trovata.**. The number of vehicles in  
 581 R1 ranged from 922 to 1 108 vph on rural roads. The difference in the number of vehicles  
 582 on urban area (from 1 276 to 780 vph) was due to the fact that a portion of traffic diverted  
 583 from R1 to the downtown city center. Field results suggest that the R3 traffic volumes are  
 584 three times higher than R2 values. This happens because R3 serves through-traffic  
 585 between Northbound and Southbound, and it is the main interchange for Eastbound-  
 586 Westbound traffic. It is worth to notice that HDV represented nearly 3%, 4% and 9% of R1,  
 587 R2 and R3 traffic composition, respectively, in the studied location.

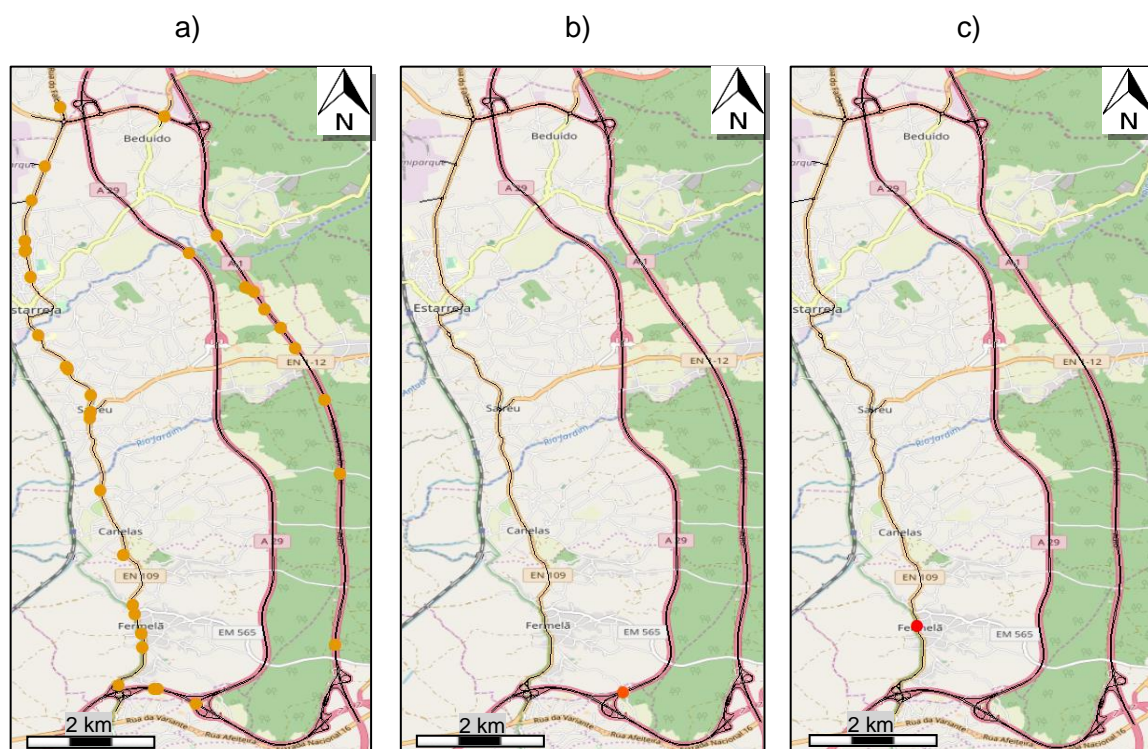


588

589 **FIGURE 5** Traffic Volumes between 5:30-6:00PM. Background Map Source [Open Street  
 590 Maps].

591

592 **Errore. L'origine riferimento non è stata trovata.** depicts the spatial distribution of 68  
 593 crashes, which took into account the level of injury severity (95 light injuries; 1 serious injury  
 594 and 1 fatality). Several conclusions about the crash database can be drawn: 1)  
 595 approximately 47% of crashes occurred in rural trip sections which corresponds to 42% of  
 596 the travel distance across the corridor; 2) albeit short, urban section had 11 crashes  
 597 involving motor vehicles, which was about 16% of crash occurrences in only 6% of overall  
 598 study domain length; 3) 49% and 37% of light injuries were observed in highway and rural  
 599 trip sections, respectively; 4) R1 had both the highest number of crash observations (41)  
 600 and highest number of light injuries (47), and it also recorded one fatal crash; and 5) main  
 601 blackspots were located in influence area of roundabouts and traffic lights along R1 (e.g.,  
 602 segments 2-17, 3-16, 4-15 and 8-9) and R3 highway trip sections (e.g., segments 9-20).



603

604 **FIGURE 6** Spatial distribution of crashes based on level of injury severity: a) Light injury; b)  
 605 Serious Injury; and c) Fatality. Background Map Source [Open Street Maps].

606

## 607 5.2. Calibration and Validation

608 The statistical indicators of the modeling platform showed solid results. For traffic, the  
 609 calibration target suggested in the literature was accomplished, i.e., GEH was lower than 4  
 610 in 39 out of 42 monitoring points (93%) (Yu and Fan, 2017). It should be emphasized that  
 611 HDV traffic distributions were used in the traffic modeling.

612 The comparison of simulated and training travel time was performed using 30 floating car  
 613 runs. The relative difference in average travel time was lower than 5% ( $p$ -value  $> 0.05$ , and  
 614 thus, not statistically significant), as shown in **TABLE 3**. During calibration, vehicle speed  
 615 distributions, critical headways at roundabouts, and green times and cycle length at traffic  
 616 lights were adjusted to fit travel time data. The comparison of testing and estimated travel  
 617 time sets also demonstrated good degree of consistency (1-6%, depending on the route);  
 618 no route showed significant differences at a 95% confidence level ( $p$ -value between 0.10  
 619 and 0.67).

620

621 **TABLE 3** Summary of Calibration and validation of travel times

Model	Route	Observed Travel Time [s]	Simulated Travel Time [s]	$p$ -value
Calibrated (Training Set)	N→S (R1)	984 ± 57	992 ± 50	0.78
	S→N (R1)	965 ± 64	987 ± 28	0.85
	N→S (R2)	605 ± 44	631 ± 31	0.13
	S→N (R2)	589 ± 39	606 ± 16	0.26
	N→S (R3)	732 ± 29	745 ± 38	0.37
	S→N (R3)	760 ± 32	784 ± 33	0.11
Validated (Testing Set)	N→S (R1)	968 ± 67	950 ± 23	0.58
	S→N (R1)	997 ± 124	1,018 ± 23	0.69
	N→S (R2)	585 ± 23	620 ± 14	0.16
	S→N (R2)	611 ± 15	608 ± 14	0.76
	N→S (R3)	752 ± 20	758 ± 26	0.73
	S→N (R3)	760 ± 4	608 ± 18	0.10

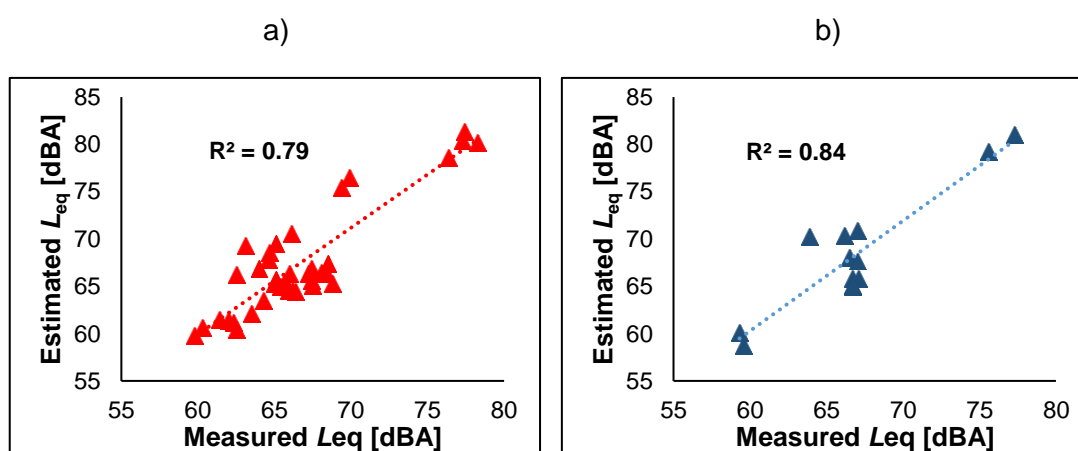
*Note:* N→S North to South; S→N South to North

622

623 It was also found that the noise estimates using the proposed methodology (Quartieri et  
 624 al., 2010) matched the field measurements (training test). Under high noise values, the



625 model tends to overestimate experimental data. This happens because field measurements  
 626 taken at bridges end up being affected by a screening due to the bridge itself, even  
 627 considering diffraction, i.e., noise emitted by vehicles outside the viewing angle of sound  
 628 level meter. The predicted coefficient of determination ( $R^2$ ) was almost 80% for simulated  
 629  $L_{eq}$  using a linear regression analysis (**Errore. L'origine riferimento non è stata trovata.**a-  
 630 b). An identical trend was observed for noise validation (testing set fit simulated data in  
 631 84%).



632

633 *Note* –  $p$ -value of  $F$ -test (ANOVA) performed in  $R^2$  coefficient was 0 in both linear regression models,  
 634 indicating statistical significance; estimated values were computed by adopting an average acoustic  
 635 equivalent ( $n$ ) value of 8.

636 **FIGURE 7** Noise methodology: a) Calibration; b) Validation.

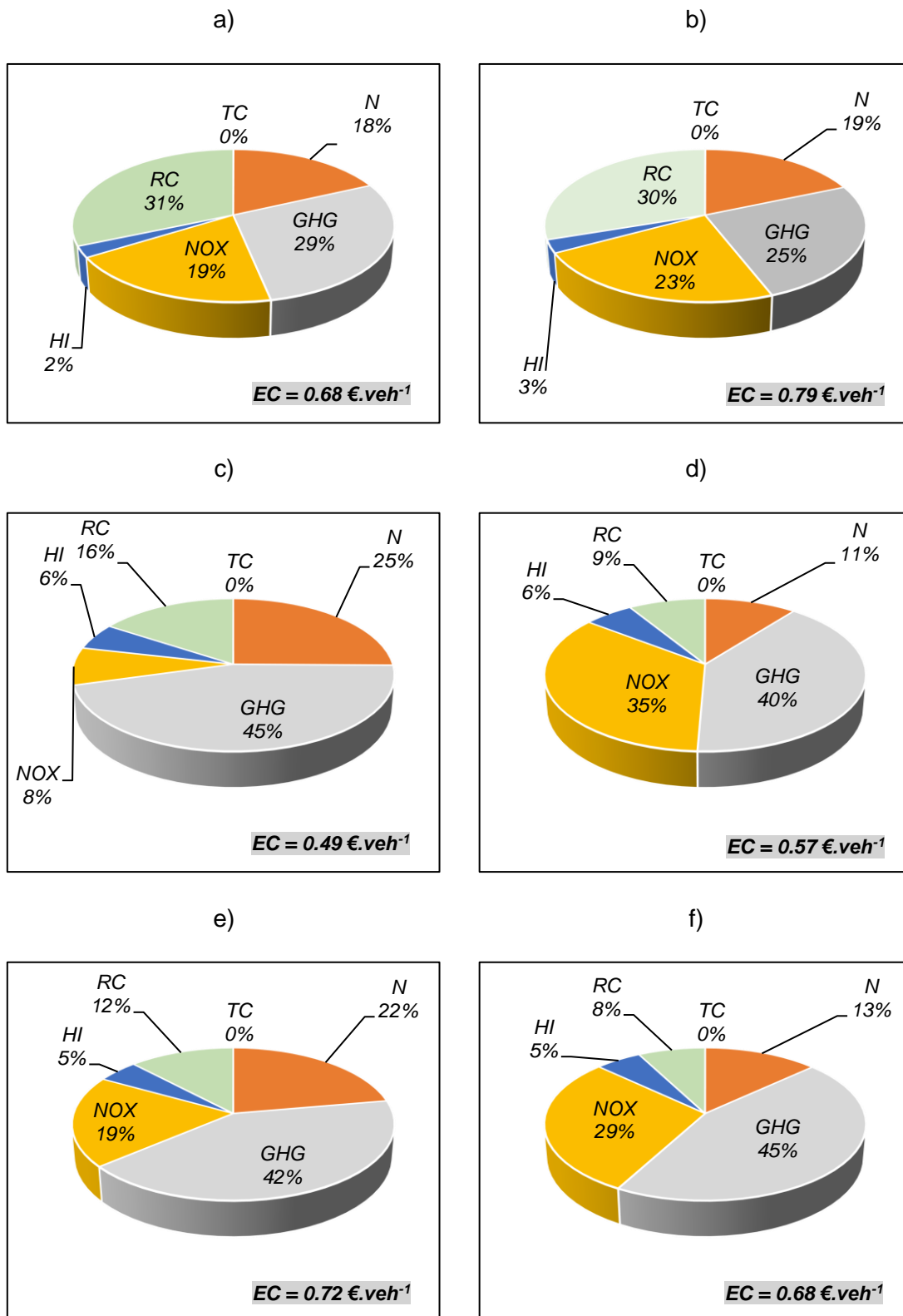
637

### 638 5.3. External Costs

639 This section presents the main results regarding external costs associated to the road traffic  
 640 with existing conditions. The sum of each segment costs ( $EC$ ) along each route confirmed  
 641 R2 as the best option for the study domain (**Errore. L'origine riferimento non è stata**  
 642 **trovata.** a-f). For instance, if one driver chooses R2 from south to north direction, then one  
 643 could save 28% and 32% in external costs when compared with R1 and R3, respectively.  
 644 Since vehicles were subjected to stop-and-go situations at conventional pay tolls (impact  
 645 on emissions as demonstrated by **Coelho et al. (2005)** together with moderate traffic

646 volumes in some of its segments, high external costs were observed for R3. For instance,  
647 segment with pay tolls accounted for approximately 10% of route external costs.

648 The analysis of the distribution of cost components along R1 showed the largest share  
649 corresponded to the RC-related costs; they represented around 31% and 30% of external  
650 costs in south-north and north-south directions, respectively. *GHG* showed as the largest  
651 contributor to external costs (40-45%, depending on travelling direction) in R2. For the latter  
652 route, results indicated the share of *RC* in south-north direction (16%) was higher than in  
653 north-south (9%). This happened because one crash involving a serious injury was  
654 recorded in segment 4, resulting thus in high social costs (see **Section 4.4** for those details).  
655 Almost half of external costs along R3 were based on *GHG* emissions, and more than 18%  
656 based on *NO<sub>x</sub>*. This was due to the fact HDV traffic is relevant in that route. In turn, other  
657 externalities (*HI* and *TC*) had slight impacts.



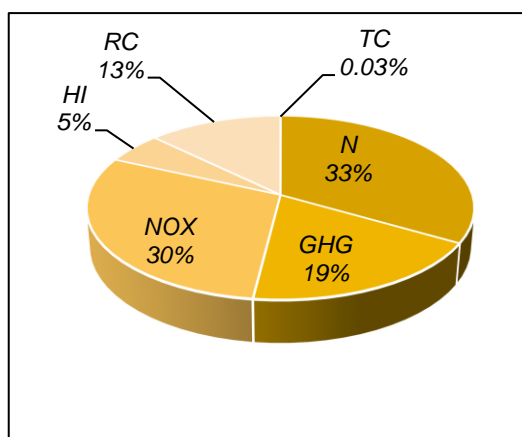
658

659 **FIGURE 8** Distribution of external costs by route: a) South to North (R1); b) North to South  
 660 (R1); c) South to North (R2); d) North to South (R2); e) South to North (R3); f) North to  
 661 South (R3).

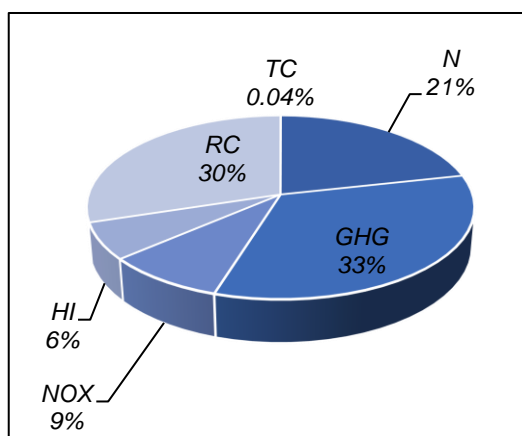
662

663 The distribution of cost components differed from the type of road (**Errore. L'origine**  
664 **riferimento non è stata trovata.** a-c). The highest share of external costs per vehicle,  
665 which was about 33% of traffic-related costs in urban sections, was due to noise generated  
666 by road traffic. This happened because  $N$  is very sensitive to changes in potentially exposed  
667 population, which is clearly high in urban segments. Albeit small,  $NO_x$  and  $PM_{10}$   
668 represented together 35% of costs in urban areas thereby, reflecting its impacts on local  
669 population. The findings from rural sections suggested a different trend ( $GHG$  accounted  
670 for 33% of external costs, followed by  $RC$ , with 30%). Concerning the highway, it is  
671 interesting to note that  $GHG$  represented around 74% of the external costs, while  $N$  and  
672  $NO_x$  had small impacts (~10% each). From **Errore. L'origine riferimento non è stata**  
673 **trovata.**, and as expected, traffic congestion had a small expression in external costs  
674 regardless of the type of road, which can be explained by the level of congestion along the  
675 study domain ( $L_i < 4$ ) (**Korzhenevych et al., 2014**).

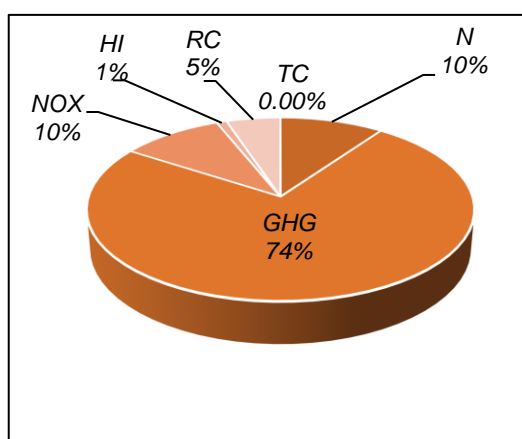
a)



b)



c)



676

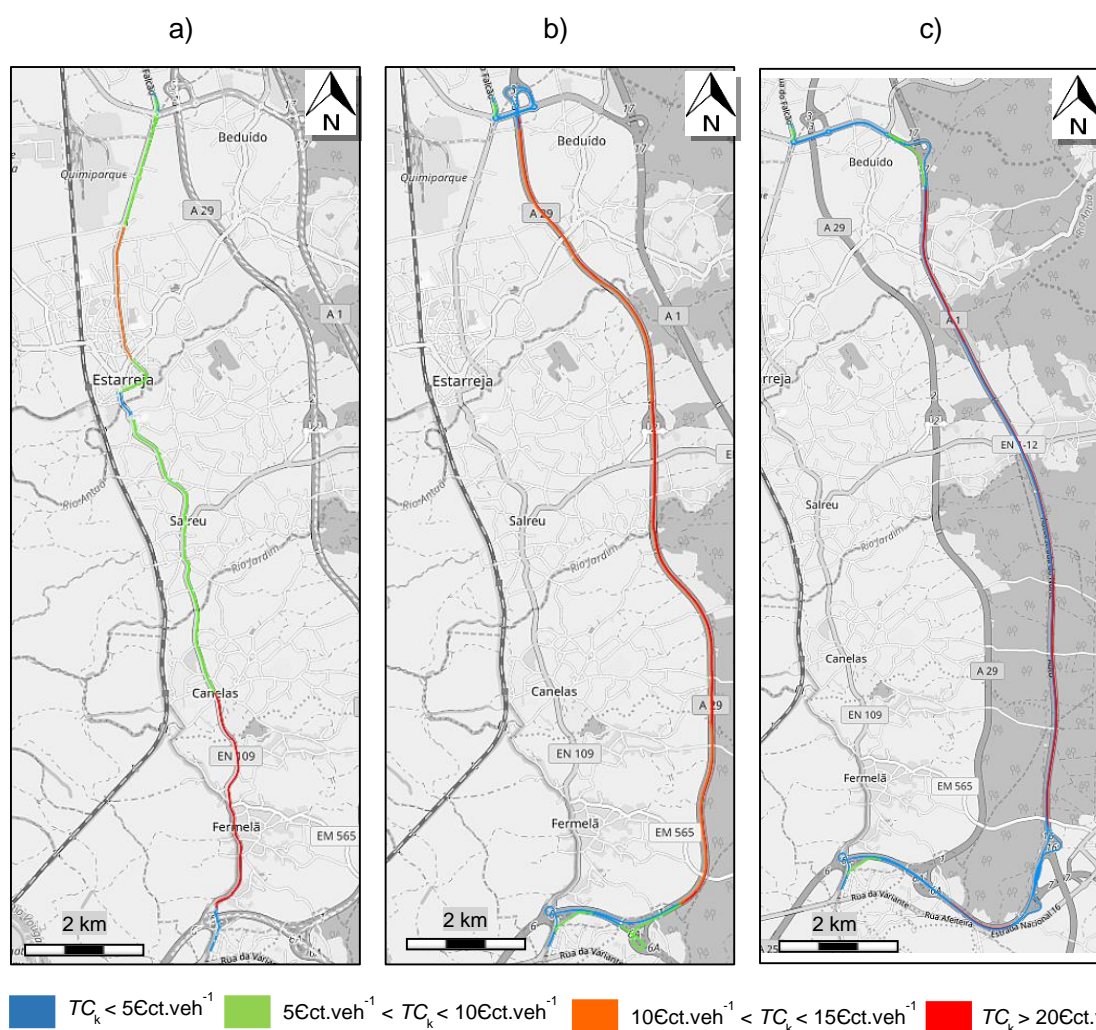
677 **FIGURE 9** Distribution of external costs by type of road: a) urban; b) rural; c) highway.

678

679 **Errore. L'origine riferimento non è stata trovata.** a-c exhibits the hotspot costs ( $TC_K$ )

680 location by segment and route. Analysis results showed links with highest costs (red color)

681 were found in segments 2-17 of R1, segments 5-12 of R2 and segments 9-20 of R3. They  
 682 represented nearly 27%, 39% and 28% of the R1, R2 and R3 total costs, respectively. The  
 683 different colors observed in North-South and South-North directions along R2 and R3 was  
 684 due to the difference in the number of crashes. Rural segments had high costs contributing  
 685 thus with 62% of total costs along R1, which was mostly explained by the number of crash  
 686 observations and resulting injury severity at those segments.



688 **FIGURE 10** Distribution of external costs by route: a) R1; b) R2; and c) R3.

689

690 The learning gained from the test of the proposed sustainability indicator in the real-world  
 691 case study is promising, which makes possible its integration in current eco-routing systems  
 692 using the methodology of this paper and apply it to any route. The sustainability indicator

693 was capable of reflecting each externality weight in costs and identifying trade-off  
694 concerning the selection of different routes with different purposes. On the one side, if  
695 drivers are guided to a route with less GHG emissions, they can be guided to roads with  
696 higher noise or air quality levels, confirming thus, the relevance for a quantification of  
697 potential population exposure. On the other side, a faster route (e.g., R3) may not represent  
698 lower external costs when compared to a slower one, emission and road crashes costs  
699 could be significant in some of its stretches when levels of traffic flows are significant. In  
700 these circumstances, the eco-routing information should be provided for ensuring both  
701 marginal private and social costs.

702

## 703 6. CONCLUSIONS

704 .The integration of road traffic impacts in one single indicator was one major drawback for  
705 the use of advance traffic management systems for estimating external costs. This paper  
706 developed a sustainability indicator for quantifying traffic externalities as means of traffic  
707 congestion, noise, GHG, NOX, health impacts and road crash related costs. The proposed  
708 methodology was tested in a commuting corridor with three main alternative routes.

709 Low-traffic-volume highway yielded 28% and 32% lower external costs than other routes.

710 Road crash costs presented the largest share along the partly rural/urban route while GHG  
711 costs were most significant in routes with highway trip sections. For the road-level analysis,  
712 some differences in the distribution of external costs can be highlighted. The share of noise  
713 and NOX in external costs were only significant in urban roads mostly due to higher  
714 potentially exposed population in those areas.

715 This research has both scientific and societal contributions. Regarding the scientific  
716 contribution, it allows incorporating other variables to assess their impact on the magnitude  
717 and share of traffic externalities according to the type of road. Some of these include the  
718 variation in the number of circulating lanes, posted speed limits, traffic control treatment

719 design, emission limit values, car fleet distributions or meteorological forecasts. Regarding  
720 the societal contribution, it allows endowing current navigation platforms with reliable and  
721 flexible cost analysis that accommodate local-specific needs and encouraging the design  
722 of eco-traffic management policies considering the perspective of drivers, commuters,  
723 population and system.

724 Undoubtedly, given the complexity of the proposed integrated approach, which alludes to  
725 areas of large-size transportation modeling, short time analysis, pollutant emissions, noise  
726 and concentrations calculations, potentially population affected to some traffic externalities,  
727 and size of crash database, several simplifications were made. These, in turn, yield three  
728 main limitations of the paper. First, on-road exposure can reach a substantial share in noise,  
729 NOX and health impact costs, but the approach in this paper assumed a fixed value (local  
730 population density). This may yield a bias in the actual and average exposure population  
731 which can vary along the day (e.g., high in urban areas during working hours, low after  
732 working hours). Second, the saturation values adopted for urban roads discarded the  
733 impacts of downstream intersections since segment-specific length was large. Since  
734 capacity is influenced by a downstream intersection in short segments, the incorporation of  
735 capacity models according to the traffic control operational characteristics (e.g., traffic light,  
736 conventional roundabouts, stop-controlled intersections) would be useful. Third, the  
737 analysis of indicator based on one hour with no variations in turning split distributions among  
738 routes. This may not represent in deep the magnitude of each cost component. Thus, the  
739 analysis of different time periods (e.g., covering all 24 h of a week) would improve the  
740 quantification of each externality.

741 Future research will be mostly focused on the use of the upcoming 5G technologies to  
742 couple the traffic information with impacts modeling analysis and crowdsourcing technology  
743 for tuning real-time potential exposure values during different periods of the day. Testing of  
744 the developed sustainability indicator in metropolitan corridors with high traffic volumes and  
745 vehicle compositions variations, and population exposure could be useful to identify



746 differences among traffic externalities. Furthermore, the incorporation and optimization of  
747 corridor-specific pricing strategies (e.g., pay tolls) on costs would also be addressed. The  
748 sustainability indicator developed in this paper assumed an equal weight for all cost  
749 components which may not correspond for local authorities and road users' preferences.  
750 Such aspects must be considered during the development of sustainable indicator by  
751 defining a specific weight for each external cost.

752

### 753 **ACKNOWLEDGEMENTS**

754 The authors acknowledge the Portuguese Authority for Road Safety (ANSR) for providing  
755 the data and the support of TEMA – CENTRO 01-0145-FEDER-022083; Strategical Project  
756 UID/EMS/00481/2013 (FCT-Portuguese Science and Technology Foundation); @CRUISE  
757 project (PTDC/EMS-TRA/0383/2014), funded within Project 9471 – Reforçar a  
758 Investigação, o Desenvolvimento Tecnológico e a Inovação and supported by European  
759 Community Fund FEDER; MobiWise (P2020 SAICTPAC/0011/2015), co-funded by  
760 COMPETE2020, Portugal2020 - Operational Program for Competitiveness and  
761 Internationalization (POCI), European Union's ERDF (European Regional Development  
762 Fund), and FCT; and CISMOB (PGI01611, funded by Interreg Europe Programme). This  
763 work was also financially supported by the project POCI-01-0145-FEDER-029463 (DICA-  
764 VE) and POCI-01-0145-FEDER-029679 (InFLOWence) funded by FEDER through  
765 COMPETE2020- Programa Operacional Competitividade e Internacionalização (POCI),  
766 and by national funds (OE), through FCT/MCTES. C. Sampaio also acknowledges the  
767 support of FCT for the Scholarship SFRH/BD/138746/2018. Thanks are due for the financial  
768 support to CESAM (UID/AMB/50017/2019), to FCT/MCTES through national funds, and the  
769 co-funding by the FEDER, within the PT2020 Partnership Agreement and Compete 2020.  
770 Finally, the cooperation of Toyota Caetano Auto S.A. is appreciated, which allowed the use  
771 of vehicles for data collection.

772

## 773 REFERENCES

- 774 Abou-Senna H, Radwan E, Westerlund K, Cooper CD. Using a traffic simulation model  
775 (VISSIM) with an emissions model (MOVES) to predict emissions from vehicles on a  
776 limited-access highway. *Journal of the Air & Waste Management Association* 2013;  
777 63: 819-831.
- 778 ANSR. Autoridade Nacional Segurança Rodoviária. Sinistralidade Rodoviária-Ano 2016.  
779 Annual Report (in Portuguese), 2017.
- 780 Anya AR, Roupail NM, Frey HC, Liu B. Method and Case Study for Quantifying Local  
781 Emissions Impacts of Transportation Improvement Project Involving Road  
782 Realignment and Conversion to Multilane Roundabout. 92nd Annual Meeting,  
783 Transportation Research Board, Washington, DC, 2013.
- 784 Bandeira J, Almeida TG, Khattak AJ, Roupail NM, Coelho MC. Generating Emissions  
785 Information for Route Selection: Experimental Monitoring and Routes  
786 Characterization. *Journal of Intelligent Transportation Systems* 2013; 17: 3-17.
- 787 Bandeira J, Fernandes P, Fontes T, Pereira S, Khattak A, Coelho MC. Exploring multiple eco-  
788 routing guidance strategies in a commuting corridor. *International Journal of*  
789 *Sustainable Transportation* 2018a; 12: 53-65.
- 790 Bandeira J, Guarnaccia C, Fernandes P, Coelho MC. Advanced Impact Integration Platform  
791 for Cooperative Road Use. *International Journal of Intelligent Transportation Systems*  
792 *Research* 2018b; 16: 1-15.
- 793 Bandeira JM, Pereira SR, Fontes T, Fernandes P, Khattak AJ, Coelho MC. An Eco-Traffic  
794 Management Tool. In: de Sousa JF, Rossi R, editors. *Computer-based Modelling and*  
795 *Optimization in Transportation*. Springer International Publishing, Cham, 2014, pp. 41-  
796 56.
- 797 Borrego C, Amorim JH, Tchepel O, Dias D, Rafael S, Sá E, et al. Urban scale air quality  
798 modelling using detailed traffic emissions estimates. *Atmospheric Environment* 2016;  
799 131: 341-351.
- 800 Borrego C, Lopes M, Cascão P, Amorim J, Martins H, Tavares R, et al. Urban air quality  
801 models. In: Chrysoulakis N, Castro E, Moors E, editors. *Understanding urban*  
802 *metabolism: a tool for urban Planning*. Routledge, UK, 2014, pp. p. 79-90.
- 803 Borrego C, Martins JM, Lemos S, Guerreiro C. A second generation Gaussian dispersion  
804 model: the POLARIS model. *International Journal of Environment and Pollution* 1997;  
805 8: 789-795.
- 806 Cecchel S, Chindamo D, Turrini E, Carnevale C, Cornacchia G, Gadola M, et al. Impact of  
807 reduced mass of light commercial vehicles on fuel consumption, CO2 emissions, air  
808 quality, and socio-economic costs. *Science of The Total Environment* 2018; 613-614:  
809 409-417.
- 810 Chang T-H, Tseng J-S, Hsieh T-H, Hsu Y-T, Lu Y-C. Green transportation implementation  
811 through distance-based road pricing. *Transportation Research Part A: Policy and*  
812 *Practice* 2018; 111: 53-64.
- 813 Chen G, Kauppila J. Global Urban Passenger Travel Demand and CO2 Emissions to 2050.  
814 *Transportation Research Record: Journal of the Transportation Research Board*  
815 2017; 2671: 71-79.
- 816 Ćirović G, Pamučar D, Božanić D. Green logistic vehicle routing problem: Routing light  
817 delivery vehicles in urban areas using a neuro-fuzzy model. *Expert Systems with*  
818 *Applications* 2014; 41: 4245-4258.
- 819 Coelho MC, Farias TL, Roupail NM. Measuring and Modeling Emission Effects for Toll  
820 Facilities. *Transportation Research Record* 2005; 1941: 136-144.

- 821 Coelho MC, Frey HC, Roupail NM, Zhai H, Pelkmans L. Assessing methods for comparing  
822 emissions from gasoline and diesel light-duty vehicles based on microscale  
823 measurements. *Transportation Research Part D: Transport and Environment* 2009;  
824 14: 91-99.
- 825 Costa S, Ferreira J, Silveira C, Costa C, Lopes D, Relvas H, et al. Integrating Health on Air  
826 Quality Assessment—Review Report on Health Risks of Two Major European Outdoor  
827 Air Pollutants: PM and NO<sub>2</sub>. *Journal of Toxicology and Environmental Health, Part B*  
828 2014; 17: 307-340.
- 829 Dias D, Amorim JH, Sá E, Borrego C, Fontes T, Fernandes P, et al. Assessing the importance  
830 of transportation activity data for urban emission inventories. *Transportation*  
831 *Research Part D: Transport and Environment* 2018; 62: 27-35.
- 832 EC. ExterneE - Externalities of Energy Methodology 2005 Update: European Commission,  
833 Retrieved from: [http://www.externe.info/externe\\_2006/](http://www.externe.info/externe_2006/), Accessed January 14, 2019,  
834 2006.
- 835 EC. Roadmap to a Single European Transport Area - Towards a competitive and resource  
836 efficient transport system: European Commission, Retrieved from:  
837 [https://ec.europa.eu/transport/sites/transport/files/themes/strategies/doc/2011\\_white](https://ec.europa.eu/transport/sites/transport/files/themes/strategies/doc/2011_white_paper/white-paper-illustrated-brochure_en.pdf)  
838 [\\_paper/white-paper-illustrated-brochure\\_en.pdf](https://ec.europa.eu/transport/sites/transport/files/themes/strategies/doc/2011_white_paper/white-paper-illustrated-brochure_en.pdf), Accessed November 9, 2018, 2011.
- 839 EC. Multimodal Sustainable Transport: which role for the internalisation of external costs?:  
840 European Commission - Directorate-General for Transport and Mobility (DG MOVE),  
841 Retrieved from: [https://ec.europa.eu/transport/sites/transport/files/2018-year-](https://ec.europa.eu/transport/sites/transport/files/2018-year-multimodality-external-costs-note.pdf)  
842 [multimodality-external-costs-note.pdf](https://ec.europa.eu/transport/sites/transport/files/2018-year-multimodality-external-costs-note.pdf), Accessed March 21, 2019, 2018.
- 843 EEA. EMEP/EEA air pollutant emission inventory guidebook: Exhaust emissions from road  
844 transport., 2013.
- 845 EEA. Air quality in Europe — 2017 report. European Environment Agency, No 13/2017,  
846 Copenhagen, Denmark, 2017a, pp. 11.
- 847 EEA. Publications - Transport and Environment Reporting Mechanism (TERM): European  
848 Environmental Agency, Retrieved from:  
849 [https://www.eea.europa.eu/downloads/00c37717c3e34479b874df54da0a2ac8/153296](https://www.eea.europa.eu/downloads/00c37717c3e34479b874df54da0a2ac8/1532961615/monitoring-progress-of-europes-transport.pdf)  
850 [1615/monitoring-progress-of-europes-transport.pdf](https://www.eea.europa.eu/downloads/00c37717c3e34479b874df54da0a2ac8/1532961615/monitoring-progress-of-europes-transport.pdf), Accessed October 31, 2018,  
851 2017b.
- 852 EEA. Air quality in Europe — 2018 report: European Environmental Agency, Retrieved from:  
853 <https://www.eea.europa.eu/publications/air-quality-in-europe-2018>, Accessed January  
854 14, 2019, 2018a.
- 855 EEA. Population exposure to environmental noise. European Environment Agency, Retrieved  
856 from: [https://www.eea.europa.eu/data-and-maps/indicators/exposure-to-and-](https://www.eea.europa.eu/data-and-maps/indicators/exposure-to-and-annoyance-by-2)  
857 [annoyance-by-2](https://www.eea.europa.eu/data-and-maps/indicators/exposure-to-and-annoyance-by-2), Accessed March 20, 2018b.
- 858 EI-Rashidy RAH, Grant-Muller SM. An operational indicator for network mobility using fuzzy  
859 logic. *Expert Systems with Applications* 2015; 42: 4582-4594.
- 860 EMISIA. COPERT Countries data: Retrieved from <http://emisia.com/products/copert-data>.  
861 Accessed May 16, 2017, 2017.
- 862 EPA. U.S. Transportation Sector Greenhouse Gas Emissions, 1990 –2016. : U.S.  
863 Environmental Protection Agency, Retrieved from:  
864 <https://nepis.epa.gov/Exe/ZyPDF.cgi?Dockey=P100USI5.pdf> Accessed October 31,  
865 2018, 2018.
- 866 ERSI. About ArcGIS | Mapping & Analytics Platform.: ERSI - Environmental Sistem  
867 Research Institute, Retrieved from: [https://www.esri.com/en-us/arcgis/about-](https://www.esri.com/en-us/arcgis/about-arcgis/overview)  
868 [arcgis/overview](https://www.esri.com/en-us/arcgis/about-arcgis/overview), 2016.
- 869 ERSO. Annual Accident Report 2018: European Road Safety Observatory, Retrieved from:  
870 [https://ec.europa.eu/transport/road\\_safety/sites/roadsafety/files/pdf/statistics/dacota](https://ec.europa.eu/transport/road_safety/sites/roadsafety/files/pdf/statistics/dacota/asr2018.pdf)  
871 [/asr2018.pdf](https://ec.europa.eu/transport/road_safety/sites/roadsafety/files/pdf/statistics/dacota/asr2018.pdf), Accessed February 18, 2019, 2018.

- 872 Fernandes P, Fontes T, Neves M, Pereira SR, Bandeira JM, Roupail NM, et al. Assessment  
873 of Corridors with Different Types of Intersections. *Transportation Research Record:*  
874 *Journal of the Transportation Research Board* 2015; 2503: 39-50.
- 875 Fernandes P, Teixeira J, Guarnaccia C, Bandeira JM, Macedo E, Coelho MC. The Potential of  
876 Metering Roundabouts: Influence in Transportation Externalities. *Transportation*  
877 *Research Record* 2018; 2672: 21-34.
- 878 Fontes T, Fernandes P, Rodrigues H, Bandeira JM, Pereira SR, Khattak AJ, et al. Are HOV/eco-  
879 lanes a sustainable option to reducing emissions in a medium-sized European city?  
880 *Transportation Research Part A: Policy and Practice* 2014; 63: 93-106.
- 881 Fries R, Qi Y, Leight S. How Many Times Should I Run the Model? Performance Measure  
882 Specific Findings from VISSIM Models in Missouri. 96th Annual Meeting of the  
883 *Transportation Research Board*, Washington, DC, 2017.
- 884 Friesz TL, Bernstein D, Kydes N. Dynamic Congestion Pricing in Disequilibrium. *Networks*  
885 *and Spatial Economics* 2004; 4: 181-202.
- 886 Guarnaccia C. Advanced Tools for Traffic Noise Modelling and Prediction. *WSEAS*  
887 *Transactions on Systems* 2013; 12: 121-130.
- 888 HCM. Highway Capacity Manual, Sixth Edition: A Guide for Multimodal Mobility Analysis,  
889 *Transportation Research Board*, Washington DC, 2016.
- 890 Hu J, Frey HC, Washburn SS. Comparison of Vehicle-Specific Fuel Use and Emissions Models  
891 Based on Externally and Internally Observable Activity Data. *Transportation Research*  
892 *Record* 2016; 2570: 30-38.
- 893 IMT. Relatório de Tráfego na Rede Nacional de Auto-Estradas [In Portuguese]: Portuguese  
894 Institute for Mobility and Transport, Retrieved from: [http://www.imt-  
895 ip.pt/sites/IMTT/Portugues/InfraestruturasRodoviaras/RedeRodoviaria/Relatrios/Rel  
896 at%C3%B3rio%20de%20Tr%C3%A1fego%20-%  
897 %204%C2%BA%20Trimestre%20de%202011.pdf](http://www.imt-ip.pt/sites/IMTT/Portugues/InfraestruturasRodoviaras/RedeRodoviaria/Relatrios/Relat%C3%B3rio%20de%20Tr%C3%A1fego%20-%204%C2%BA%20Trimestre%20de%202011.pdf), November 11, 2018, 2011.
- 898 IMT. Relatório de Tráfego na Rede Nacional de Auto-Estradas [In Portuguese], Portuguese  
899 Institute for Mobility and Transport: Portuguese Institute for Mobility and Transport,  
900 Retrieved from: [http://www.imt-  
901 ip.pt/sites/IMTT/Portugues/InfraestruturasRodoviaras/RedeRodoviaria/Relatrios/Rel  
902 at%C3%B3rio%20de%20Tr%C3%A1fego%20-%  
903 %204%C2%BA%20Trimestre%20de%202018.pdf](http://www.imt-ip.pt/sites/IMTT/Portugues/InfraestruturasRodoviaras/RedeRodoviaria/Relatrios/Relat%C3%B3rio%20de%20Tr%C3%A1fego%20-%204%C2%BA%20Trimestre%20de%202018.pdf), April 8, 2019, 2019.
- 904 Int Panis L, De Nocker L, Cornelis E, Torfs R. An uncertainty analysis of air pollution  
905 externalities from road transport in Belgium in 2010. *Science of The Total*  
906 *Environment* 2004; 334-335: 287-298.
- 907 Jovanović AD, Pamučar DS, Pejčić-Tarle S. Green vehicle routing in urban zones – A neuro-  
908 fuzzy approach. *Expert Systems with Applications* 2014; 41: 3189-3203.
- 909 Khan T, Frey HC. Comparison of real-world and certification emission rates for light duty  
910 gasoline vehicles. *Science of The Total Environment* 2018; 622-623: 790-800.
- 911 Kickhöfer B, Kern J. Pricing local emission exposure of road traffic: An agent-based  
912 approach. *Transportation Research Part D: Transport and Environment* 2015; 37: 14-  
913 28.
- 914 Kickhöfer B, Nagel K. Towards High-Resolution First-Best Air Pollution Tolls. *Networks and*  
915 *Spatial Economics* 2016; 16: 175-198.
- 916 Korzhenevych A, Dehnen N, Bröcker J, Holtkamp M, Meier H, Gibson G, et al. Update of the  
917 *Handbook on External Costs of Transport - Final Report*, 2014.
- 918 Liu H, Gegov A, Cocea M. Unified Framework for Control of Machine Learning Tasks Towards  
919 Effective and Efficient Processing of Big Data. In: Pedrycz W, Chen S-M, editors. *Data*  
920 *Science and Big Data: An Environment of Computational Intelligence*. Springer  
921 International Publishing, Cham, 2017, pp. 123-140.

- 922 National Academies of Sciences E, and Medicine 2018,. Critical Issues in Transportation 2019.  
923 Networks and Spatial Economics, 2018, pp. 45.
- 924 Pamučar D, Gigović L, Ćirović G, Regodić M. Transport spatial model for the definition of  
925 green routes for city logistics centers. Environmental Impact Assessment Review  
926 2016a; 56: 72-87.
- 927 Pamucar D, Goran Ćirović G. Vehicle route selection with an adaptive neuro fuzzy inference  
928 system in uncertainty conditions Decision Making: Applications in Management and  
929 Engineering 2018; 1: 13-37.
- 930 Pamučar D, Ljubojević S, Kostadinović D, Đorović B. Cost and risk aggregation in multi-  
931 objective route planning for hazardous materials transportation—A neuro-fuzzy and  
932 artificial bee colony approach. Expert Systems with Applications 2016b; 65: 1-15.
- 933 PTV AG. PTV VISSIM 9 User Manual: Planung Transport Verkehr AG, Karlsruhe, Germany,  
934 2016.
- 935 Quartieri J, Iannone G, Guarnaccia C. On the Improvement of Statistical Traffic Noise  
936 Prediction Tools. 11th WSEAS Int. Conf. on Acoustics & Music: Theory &  
937 Applications, Iasi, Romania, June 13-15, 2010, pp. 201-207.
- 938 Rivera F, Chamorro A, Lucero R, Aravena C. Development of Condition Indicator for Managing  
939 Sealed Rural Road Networks. Transportation Research Record: Journal of the  
940 Transportation Research Board 2015; 2474: 90-97.
- 941 Ruckerl R, Schneider A, Breitner S, Cyrus J, Peters A. Health effects of particulate air  
942 pollution: A review of epidemiological evidence. Inhalation Toxicology 2011; 23: 555-  
943 592.
- 944 Sampaio C, Bandeira JM, Macedo E, Vilaça M, Guarnaccia C, Friedrich B, et al. A Dynamic  
945 Link-based Eco-indicator for supporting equitable traffic management strategies.  
946 Transportation Research Procedia 2019; 37: 43-50.
- 947 Sdoukopoulos A, Pitsiava-Latinopoulou M, Basbas S, Papaioannou P. Measuring progress  
948 towards transport sustainability through indicators: Analysis and metrics of the main  
949 indicator initiatives. Transportation Research Part D: Transport and Environment  
950 2019; 67: 316-333.
- 951 Small KA, Verhoef ET. The Economics of Urban Transportation: Routledge, 2007.
- 952 Statistics of Portugal. Resident persons (No.) in family nuclei by Place of residence: Retrieved  
953 from: <https://ine.pt>. Accessed July 12, 2017, 2018.
- 954 Tafidis P, Sdoukopoulos A, Pitsiava-Latinopoulou M. Sustainable urban mobility indicators:  
955 policy versus practice in the case of Greek cities. Transportation Research Procedia  
956 2017; 24: 304-312.
- 957 Torrao G, Fontes T, Coelho M, Roupail N. Integrated indicator to evaluate vehicle  
958 performance across: Safety, fuel efficiency and green domains. Accident Analysis &  
959 Prevention 2016; 92: 153-167.
- 960 Turner S. Travel Time Data Collection Handbook: Office of Highway Information Management,  
961 Federal Highway Administration, U.S. Department of Transportation, 1998.
- 962 US EPA. Methodology for developing modal emission rates for EPA's multi-scale motor  
963 vehicle & equipment emission system, 2002.
- 964 Valente J, Pimentel C, Tavares R, Ferreira J, Borrego C, Carreiro-Martins P, et al. Individual  
965 Exposure to Air Pollutants in a Portuguese Urban Industrialized Area. Journal of  
966 Toxicology and Environmental Health, Part A 2014; 77: 888-899.
- 967 Vasconcelos L, Seco A, Silva AB. Comparison of Procedures to Estimate Critical Headways  
968 at Roundabouts. Promet - Traffic and Transportation 2013; 25: 43-53.
- 969 Vlachokostas C, Achillas C, Moussiopoulos N, Kalogeropoulos K, Sigalas G, Kalognomou E-  
970 A, et al. Health effects and social costs of particulate and photochemical urban air

- 971 pollution: a case study for Thessaloniki, Greece. *Air Quality, Atmosphere & Health*  
972 2012; 5: 325-334.
- 973 WHO. Burden of disease from environmental noise - Quantification of healthy life years lost  
974 in Europe: World Health Organization, Retrieved from:  
975 [http://www.euro.who.int/data/assets/pdf\\_file/0008/136466/e94888.pdf](http://www.euro.who.int/data/assets/pdf_file/0008/136466/e94888.pdf), Accessed  
976 February 2, 2019, 2011.
- 977 Winnie D, Christine B, Serge P. H. *Traffic Simulation and Data: Validation Methods and*  
978 *Applications*: CRC Press, Taylor & Francis Group, Boca Raton, FL, 2014.
- 979 Yeh C-F. Evaluation methods for external costs for road traffic based on objective  
980 territorialization in the metropolis. *Cities* 2013; 31: 76-84.
- 981 Yu M, Fan W. Calibration of microscopic traffic simulation models using metaheuristic  
982 algorithms. *International Journal of Transportation Science and Technology* 2017; 6:  
983 63-77.
- 984